Point Mutations of Weak Lysine Binding Sites in Apolipoprotein(a): Effects on Lp(a) Assembly

By

THEODORE G. WRIGHT

A thesis submitted to the Department of Biochemistry in accordance with the requirements for the degree of Master of Science

Queen's University
Kingston, Ontario, Canada
December, 2000

Abstract

The process of Lp(a) assembly occurs in two steps, wherein initial non-covalent association of apo(a) and apoB precedes specific disulfide linkage. The non-covalent association is sensitive to the addition of lysine and proline, and involves sequences within apo(a) kringle (K) IV_{6-8}. In the present study, we have utilized site-directed mutagenesis to specifically study the contribution of the weak lysine binding sites (WLBS) in apo(a) KIV types 6,7 and 8 to non-covalent interactions with apoB. We introduced a Glu to Gly substitution in each of the KIV types 6,7 and 8 as well as simultaneously mutating WLBS in KIV types 6 and 7 and KIV types 7 and 8. All mutants were generated in the context of a 17-kringle recombinant apo(a) and were used to transfect human embryonic kidney cells. Apo(a) derivatives were purified from the conditioned media by lysine-Sepharose affinity chromatography. Purified proteins were assessed for their ability to bind to fluorescently-labeled human LDL in solution. Analysis of binding affinities demonstrated that removal of the WLBS in KIV_7 had little or no effect on the interaction, while 2- and 4-fold decreases in affinity were observed upon removal of the WLBS in KIV types 7 and 8, respectively. Simultaneous removal of the WLBS in KIV types 6 and 7 reduced the affinity for the LDL by approximately 3-fold, while a 13-fold decrease in affinity was observed upon simultaneous removal of the WLBS in KIV types 7 and 8. The derivatives described above were also assessed for their effect on covalent Lp(a) assembly by SDS-PAGE under non-reducing conditions followed by Western blotting. Trends observed in the non-covalent binding were

paralleled in this analysis; the greatest effect on both maximum Lp(a) formation over 24 hours (~50% decrease) and rate of particle assembly (~70% decrease) was observed using the derivative with the WLBS in both KIV types 7 and 8 removed. Taken together, our data suggest that the WLBS in both apo(a) KIV types 7 and 8 are required for non-covalent association with apoB, and that the efficiency of the first step of Lp(a) formation dictates the extent to which covalent Lp(a) particles are formed.

Acknowledgements

First and foremost, I would like to thank my supervisor Dr. Marlys L. Koschinsky for giving me the opportunity to work in her lab and for all of the guidance throughout this project. Also, I extend my gratitude to members of the Koschinsky lab, past and present, for their great guidance and wonderful friendship. I especially appreciate the training in various laboratory techniques received from Dr. Brent Gabel and the knowledge and assistance in the construction of the apo(a) constructs from Lorraine May. I would like to thank Lev Becker for assistance with the fluorescence binding assays as well as numerous other instances of help and insight. Dr. Michael Nesheim was extremely helpful in the analysis of the fluorescent binding data and I am thankful. I would also like to thank the Canadian Institutes of Health Research for funding of this project.

I would like to thank all of the people, here and at home, who lent me their ears when needed and offered their friendship. Lastly, I want to thank my family for their encouragement and love. Thank you tonnes.

Table of Contents

2. Materials and Methods

3. Results

4. Discussion

List of Tables

List of Figures

List of Abbreviations

293	human embryonic kidney cells
6-AHA	6-amino hexanoic acid
6K r-apo(a)	6-kringle recombinant apo(a) derivative
12K r-apo(a)	12-kringle recombinant apo(a) derivative
17K r-apo(a)	17-kringle recombinant apo(a) derivative
17KΔWLBS6	17-kringle apo(a) containing Glu56→Gly56 substitution in KIV_6
17KΔWLBS7	17-kringle apo(a) containing Glu56→Gly56 substitution in KIV_7
17KΔWLBS8	17-kringle apo(a) containing Glu56→Gly56 substitution in KIV_8
17KΔWLBS6,7	17-kringle apo(a) containing Glu56→Gly56 substitutions in KIV_6 and KIV_7
17KΔWLBS7,8	17-kringle apo(a) containing Glu56→Gly56 substitutions in KIV_7 and KIV_8
AB5-33A	sheep polyclonal capture antibody
anti-apo(a)	goat anti-human apo(a) anti-serum
apo(a)	apolipoprotein (a)
apoB	apolipoproteinB
bp	base pair(s)
BSA	bovine serum albumin
C-	carboxyl
CHD	coronary heart disease
CHO	Chinese hamster ovary cells
CM	conditioned media
COS	*C. aethiops* kidney cells
DEAE	diethylaminoethylene anion-exchange column
DNA	deoxyribosenucleic acid
ε-ACA	ε-aminocaproic acid
E. coli	*Escheria coli*
EDTA	ethylenediamine tetraacetate
ELISA	enzyme-linked immunosorbant assay
ER	endoplasmic reticulum
FCS	fetal calf serum
Flu-LDL	5'-IAF labeled LDL
g	gravitational force
G418	Geneticin antibiotic
HBS	HEPES buffered saline, pH 7.4
HBST	HBS containing 0.01% (v/v) Tween-20
HEPES	*N*-(2-hydroxyethyl)piperazine-*N'*-(2-ethanesulfonic acid)
HepG2	human hepatocellular carcinoma
hr	hour(s)
IAF	iodoacetamidofluorescein

IDL	intermediate density lipoprotein
IgG	immunoglobulin G
K	kringle domain
K_d	dissociation constant
kDa	kilo Dalton
KIV_n	apo(a) kringle IV type n domain(s)
KIV_{n-P}	apo(a) kringle IV type n to P domains
KV	apo(a) kringle V domain
LBS	lysine binding site(s)
LDL	low density lipoprotein
Lp(a)	lipoprotein(a)
M	moles/Litre
Mab-34	anti-apo(a) monoclonal antibody specific for protease domain
MBN	mung bean nuclease
McA-Rh7777	rat hepatocytes
MEM	minimal essential medium
min	minute(s)
MW	molecular weight
N-	amino
NET	NaCl/EDTA/Tris/Triton, pH 7.4
OptiMEM	serum free MEM
P	protease domain
PBS	phosphate buffered saline, pH 7.4
PBST	PBS containing 0.1% (v/v) Tween-20
PCR	polymerase chain reaction
PDI	protein disulfide isomerase
PMSF	phenylmethylsulfonylfluoride
rpm	revolutions per minute
S	signal sequence
SDS-PAGE	sodium dodecyl sulfate polyacrylamide gel electrophoresis
T	tail region
TE	Tris buffered saline, containing 1 mM EDTA, pH 7.4
TGF-β	transforming growth factor beta
tPA	tissue-type plasminogen activator
uPA	urokinase-type plasminogen activator
VLDL	very low density lipoprotein
WLBS	weak lysine binding site(s)

Preface

This thesis was written in accordance with regulation 8.6a of the Queen's University School of Graduate Studies and Research Handbook (2000-2001).

Introduction

1.1 Overview

Lipoprotein(a) [Lp(a)] antigen was first detected by Kåre Berg (1) in human plasma and was described as a qualitative genetic trait [either Lp(a)+ or Lp(a)-]. As detection methods improved it became clear that plasma concentrations of Lp(a) are a quantitative trait and concentrations range in the human population from <0.1 mg/dl to >100 mg/dl. (2) In addition to humans, Lp(a) is also present in a limited number of other species, including higher primates and hedgehogs. (3) Lp(a) remains a focus of research interest due to the epidemiological studies that have correlated high Lp(a) levels (greater than a risk threshold of 20-30 mg/dl) with an increased risk of development of atherosclerotic disorders, including coronary heart disease (CHD). (2,4,5)

1.2 Structure of Lp(a) Particles

Lp(a) contains two components, a low density lipoprotein (LDL)-like particle and the highly glycosylated apolipoprotein(a) [apo(a)] moiety (see Figure 1.1). (6,7,8) The LDL-like moiety of Lp(a) consists of the apolipoprotein B-100 protein (4536 amino acids) closely associated with the cholesterol and phospholipids on the surface of the particle, whose lipid core is composed of cholesterol esters and triglycerides. (9,10,11,12,13) ApoB-100 consists of five different sub-domains (I-V), as evidenced by thermal unfolding occurring in a step-wise manner relatively independent of each other, with the C-terminal domain (V) being the most hydrophobic. (13,14) ApoB-100 contains

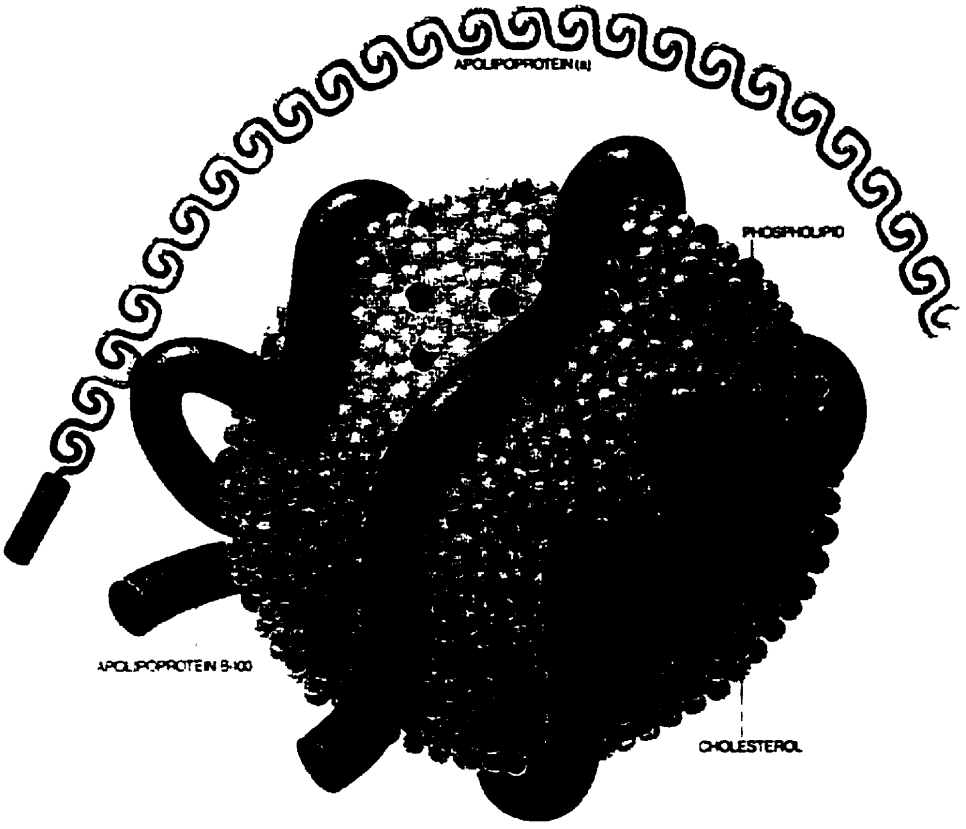

Figure 1.1

Schematic representation of the Lp(a) particle. The LDL-like moiety consists of the apolipoprotein B-100 protein closely associated with the cholesterol and phospholipids on the surface of the core lipid particle. This LDL-like moiety is attached by a single disulfide bond to the glycoprotein apolipoprotein(a) in the Lp(a) particle.
[Lawn, R.M. (1992) *Sci. Am.* 266:54-60]

25 cysteines that are concentrated in the N-terminus, of which 16 are involved in 8 intra-molecular disulfide bonds. (13,15) Of the seven remaining cysteines, two, located at the C-terminus, are on the surface of LDL making them available for disulfide linkage to apo(a) to form Lp(a) particles. (16,17) The identity of the apoB-100 cysteine responsible for disulfide linkage to the cysteine on apo(a) remains controversial (see Section 1.5.4).

Lp(a) is distinquished from LDL by the presence of the glycoprotein apo(a) (see Section 1.4), which is attached by a single disulfide bond to apoB-100; the apo(a) and apoB100 are in a 1:1 molar ratio in the Lp(a) particle. (18) Lp(a) can be detected in human plasma using antibodies specific for either apo(a) or LDL. (2) Lp(a) can be found in human plasma at a density between 1.02 g/ml to 1.10 g/ml, depending on the apo(a) isoform size (ranging from 200 to 800 kDa; see Section 1.4) as well as the lipid composition of the LDL component. (10) The apo(a) component of Lp(a) contains multiple domain repeats known as kringles (see Figure 1.2). Kringles are common in plasma proteins involved in the coagulation and fibrinolytic cascades, where they likely mediate specific binding functions. (4) Lp(a) shares characteristics with both LDL and apo(a) and as such, the pathogenicity of Lp(a) may be attributed to either, or both of these components (see Section 1.3).

1.3 Lipoprotein(a) as a Risk Factor for Coronary Heart Disease

The majority of epidemiological studies performed over the past three decades suggest that elevated plasma levels of Lp(a) confer an increased risk for the development of atherosclerotic disorders including coronary heart disease (CHD). (2,4) Lp(a)

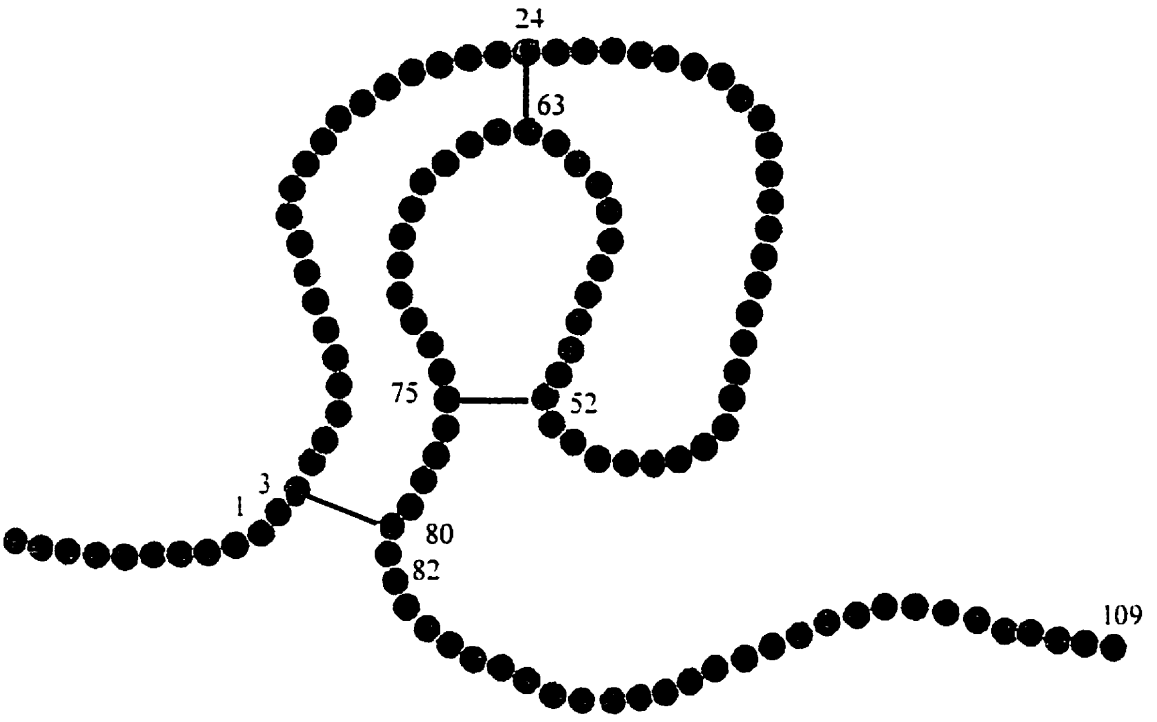

Figure 1.2

General representation of a tri-looped kringle structure. A kringle consists of approximately 80 amino acids (1-82), of which six cysteines are paired to form three intra-kringle disulfide bonds. In apo(a), multiple kringles are separated by an inter-kringle domain of approximately 30 amino acids (83-109)

accumulates in the arterial intima at the sites of atherosclerotic lesions, to an extent that is proportional to plasma Lp(a) concentration. (2,19,20,21) Whether this accumulation is a cause or consequence of CHD is unclear, however. The apo(a) component of Lp(a) is highly polymorphic (see Section 1.4), which complicates the design and interpretation of epidemiological studies.

The role of Lp(a) in CHD may reflect its similarity to the atherogenic LDL particle. LDL can be modified *in vitro* by chemical acetylation or oxidation to a form that is recognized and internalized by monocyte/macrophage scavenger receptors; *in vitro* studies suggest that the LDL-component of Lp(a) can be modified in a similar manner (26) Once this uptake occurs accumulation of modified LDL results in the conversion of macrophages into foam cells. (27) Foam cells are macrophages that have collected beneath the vascular endothelium and have been loaded with cholesterol esters. (28) Compared to LDL, Lp(a) preferentially accumulates in the intima of vessel walls by interactions with numerous extracellular matrix components including glycosaminoglycans, fibronectin, fibrinogen and fibrin. (4) As mentioned above, once entrapped in the vessel wall the LDL component of Lp(a) may undergo oxidative modification. Like modified LDL, this oxidized Lp(a) can also be a ligand for the macrophage scavenger receptor, thereby contributing to foam cell formation. (4)

The similarity of the apo(a) component of Lp(a) to plasminogen (see Section 1.4, Figure 1.3) has been proposed to result in the ability of Lp(a) to interfere with the normal functions of plasminogen. Plasminogen is a zymogen that is cleaved by plasminogen activators such as urokinase-type plasminogen activator (uPA) or tissue-type plasminogen

activator (tPA), to generate active plasmin. (7,29) Plasmin in turn cleaves fibrin, thereby resulting in the dissolution of fibrin clots. Lp(a) is able to bind to similar substrates as plasminogen including proteoglycans, fibronectin, fibrinogen and fibrin. (4) Like plasminogen, the binding of Lp(a) to some of these substrates is mediated by a strong lysine binding site (LBS) in apo(a) (see Section 1.4, Figure 1.4). (30,31) Lp(a) has been suggested to compete with plasminogen for binding to fibrinogen, thereby interfering with plasminogen activation which is essential for the normal fibrinolytic function of plasmin. This in turn has been proposed to result in the generation of a prothrombotic state *in vivo*. Lp(a) has been shown to interfere with fibrin clot lysis *in vitro* (32,33), as well as in transgenic mice overexpressing apo(a). (34) Additionally, an inverse relationship has been demonstrated between plasma Lp(a) levels and levels of active transforming growth factor beta (TGF-β) in the vessel wall. (35) This has been suggested to result from the Lp(a)-mediated inhibition of plasminogen activation, thereby resulting in a decrease in the activation of TGF-β. Normally, TGF-β is activated from its latent form by plasmin cleavage; active TGF-β inhibits smooth muscle cell proliferation and migration. Lp(a) has therefore been proposed to inhibit TGF-β activation and therefore promote smooth muscle cell proliferation and migration, which contributes to the atherosclerotic process. (2,35,36)

1.4 Structure of Apolipoprotein(a)

Apo(a) is a highly glycosylated protein (~30% carbohydrate weight) which is primarily synthesized by the liver. (37,38) Apo(a) is highly polymorphic, with at least 34

different isoforms reported to date, corresponding to proteins which range in mass from <200 kDa to >800 kDa. (11,39) The size heterogeneity of apo(a) is controlled by the polymorphic *apo(a)* gene locus. (11,40) In the Caucasian population the *apo(a)* gene is responsible for >90% of variation in Lp(a) concentrations in plasma. (11,40) As mentioned above (see Section 1.3), apo(a) shares a high degree of sequence similarity with the fibrinolytic proenzyme plasminogen. Plasminogen consists of five distinct domains known as kringles, designated K 1-5, which are followed by a C-terminal serine protease domain. (29) The protease domain can be catalytically activated by either tPA or uPA. (7,29) Apo(a) contains no sequences corresponding to plasminogen kringles 1-3, but rather has multiple copies of a kringle homologous to plasminogen kringle 4, followed by a single copy of a kringle which shares ~90% sequence identity with plasminogen kringle 5, followed by a catalytically inactive serine protease-like domain (see Figure 1.3). (7,32,41,42) The apo(a) kringle IV-like domains can be subdivided into ten distinct classes on the basis of amino acid sequence and are designated $KIV_{1\text{-}10}$ (see Figure 1.4). All apo(a) isoforms contain a single copy of KIV_1 and $KIV_{3\text{-}10}$, while differing numbers of identically-repeated KIV_2 sequences, ranging from 3 to >50, form the molecular basis of apo(a) isoform size heterogeneity. (39,43)

Apo(a) KIV domains consist of approximately 80 amino acids, which are separated by an inter-kringle region of approximately 30 amino acids. (44). All apo(a) KIV domains contain six cysteines which are paired to form three intra-kringle disulfide bonds, resulting in a characteristic tri-loop structure (see Figure 1.2). KIV_9 contains an additional seventh unpaired cysteine, which has been shown to be involved in disulfide

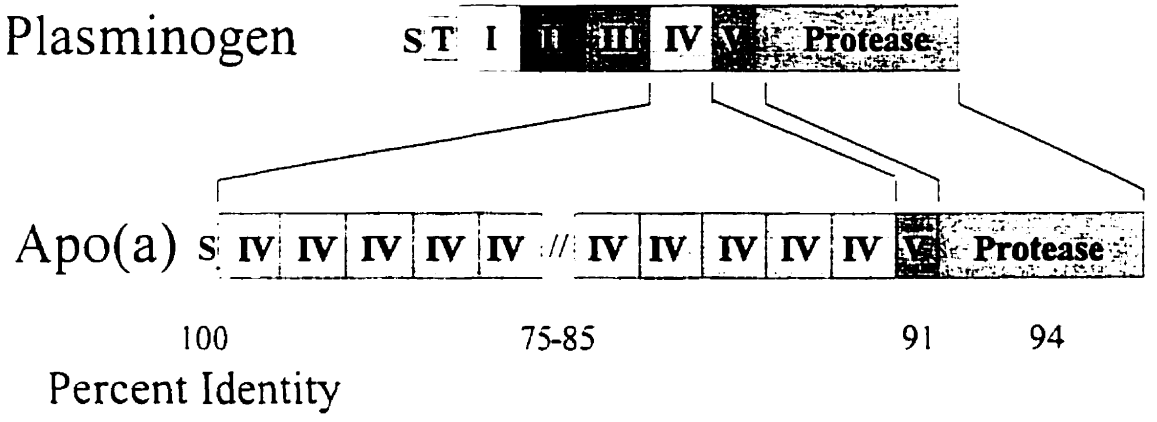

Figure 1.3

Comparison of the structure of plasminogen and apo(a). Plasminogen consists of five distinct kringle domains (K 1-5), followed by an activatable C-terminal serine protease domain. Apo(a) consists of multiple copies of a kringle 4-like domain, followed by a single copy of a kringle 5-like domain and a catalytically inactive serine protease-like domain. Amino acid sequence identity of apo(a) to plasminogen for the various domains is indicated.

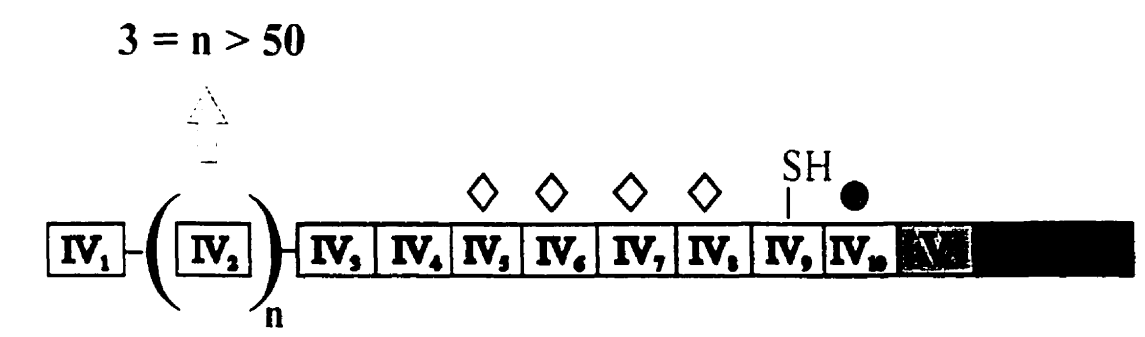

Figure 1.4

Structural organization of apo(a). Apo(a) is subdivided into ten distinct classes of kringles, designated KIV_{1-10} (types 1 to 10). All apo(a) isoforms contain a single copy of KIV_1 and KIV_{3-10}, while the number of KIV_2, repeats form the molecular basis of apo(a) isoform size heterogeneity. The weak lysine binding sites present in KIV_{5-8} are designated by diamonds. The unpaired cysteine in KIV_9, which is involved in disulfide linkage to apoB, is indicated. The strong lysine binding site in KIV_{10} is designated by a circle. The KV and inactive protease domains are located at the C-terminus of the molecule.

linkage with the apoB-100 component of LDL to form Lp(a) particles (see Section 1.5.3). (45,46) Apo(a) is highly glycosylated and has at least one *N*-glycosylation site per KIV domain and up to six *O*-glycosylation sites in each inter-kringle sequence. (47) Apo(a) is synthesized as a smaller-sized precursor in the endoplasmic reticulum (ER) (48): *N*- and *O*-linked glycosylation occurs in the ER and Golgi of hepatocytes, thereby resulting in the larger mature form observed in plasma.

KIV_{10} contains a relatively strong LBS (which is the most similar to plasminogen K4), which mediates lysine binding of Lp(a) to biological substrates. (29,30,49) Based on comparison with plasminogen K4, the KIV_{10} LBS consists of a conserved seven amino acid pocket. (49) This pocket consists of a hydrophobic trough (Trp62, Phe64, Trp72), a cationic site (Arg35, Arg71) and an anionic site (Asp55, Asp57). (44) A Trp72→Arg72 substitution phenotype in KIV_{10} has been identified in <2% of the human population which abolishes the lysine binding ability of the corresponding Lp(a) species. (50) Also, an Asp57→Asn57 substitution in KIV_{10} of chimpanzees abolishes the LBS properties of KIV_{10} and causes a decrease in apo(a) binding to fibrin. (51) KIV_{5-8} each contain a weak LBS (WLBS) which have been suggested to be required for the initial step in Lp(a) assembly (see Section 1.5). (52,53,54,55) These WLBS also consist of a conserved seven amino acid pocket (see Figure 1.5), with two modifications compared to the KIV_{10} strong LBS pocket. (44) The hydrophobic region contains Tyr64 compared to Phe64 in KIV_{10}. Also, the anionic site contains Glu57 compared to Asp57 in KIV_{10}. These changes have been predicted to cause a decrease in lysine binding ability of KIV_{5-8} compared to that of KIV_{10}.

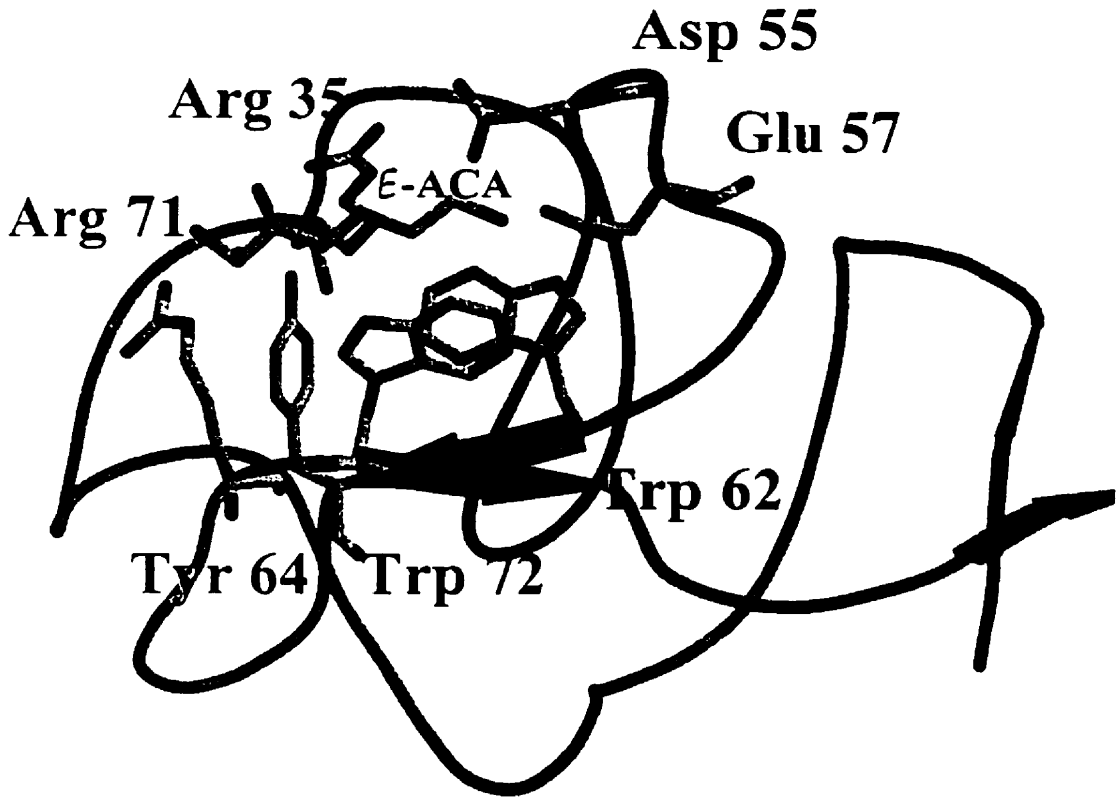

Figure 1.5

Ribbon diagram of the weak lysine binding site of KIV-, consisting of a conserved seven amino acid pocket. The pocket is formed by a cationic site consisting of Arg35 and Arg71, an anionic site consisting of Asp55 and Glu57 and a hydrophobic trough consisting of Trp62, Tyr64 and Trp72. Also modeled is the position of the lysine analogue 6-aminocaproic acid (ε-ACA). [Model kindly provided by Dr. Zongchoa Jia, Department of Biochemistry, Queen's University, Kingston, Ontario]

1.5 Assembly of Lipoprotein(a)

Although apo(a) can be synthesized and secreted from hepatocytes independently of apoB-containing lipoproteins, very little free apo(a) is found in human plasma. (45). Rather, the majority of plasma apo(a) is covalently linked to LDL. Therefore, covalent assembly of apo(a) and apoB appears to be essential for the presence of circulating Lp(a) in human plasma. As such, much work has been done to understand the process of Lp(a) formation.

1.5.1 Site of Lp(a) Assembly

ApoB-100 is produced by the liver in humans, while a truncated form of apoB, apolipoprotein B-48 (apoB-48), is produced in the human intestine. (12) ApoB-100, consisting of 4536 amino acids, is the major protein component of a number of plasma lipoproteins, including very low density lipoprotein (VLDL), intermediate low density lipoprotein (IDL) and low density lipoprotein (LDL). (13) Pulse-chase studies using human hepatocytes (HepG2) have suggested that translocation of apoB-100 across the endoplasmic reticulum (ER) lumen and lipid transfer to apoB-100 occurs co-translationally. (55,56) Apo(a) is also synthesized in the liver as demonstrated by transplantation studies. (57) A debate currently exists about the location of apo(a) and apoB-100 assembly to form Lp(a) particles. Very little free apo(a) is detectable in human plasma (45), suggesting assembly with apoB-100 prior to or immediately after secretion from liver cells. Recent studies using a recombinant 6 kringle (6K) form of apo(a) expressed in HepG2 cells demonstrated the presence of Lp(a) in cell lysates, suggesting

intracellular assembly (58), although earlier studies (46) using a 17 kringle (17K) form of r-apo(a) failed to detect an intracellular Lp(a) species. Using human liver samples, it was demonstrated that apo(a) and apoB are not associated in the liver. (59) Further studies using baboon hepatocytes reinforced the notion of extracellular Lp(a) assembly. (48,60) Co-immunoprecipitation of apoB-100 with apo(a) was inhibited by supplementation of the conditioned media (CM) from baboon hepatocytes with goat anti-human apo(a) anti-serum [anti-apo(a)], which suggested that apo(a)-apoB assembly is extracellular. Additionally the lysine analog 6-amino hexanoic acid (6-AHA) inhibited Lp(a) assembly when added to the medium of the baboon hepatocytes. (60) It has been suggested that Lp(a) assembly may occur on the surface of the hepatocytes (60); addition of 6-AHA and proline was shown to release apo(a) from the hepatocyte surface, probably by disrupting kringle interactions with the cell surface. (60) Kringles responsible for cell surface binding appear to be masked in the context of Lp(a) since addition of apo(a) and Lp(a) to cell culture show binding of apo(a), but not Lp(a) to the cell surface. Supplementation of culture medium with LDL caused the release of cell surface bound apo(a) in the form of Lp(a). Protein disulfide isomerase (PDI) in the ER is known to play a role in intra-disulfide binding of apoB which affects translocation and secretion of LDL. (61) The cell surface assembly of Lp(a) has also been suggested to be catalyzed by PDI that may be present in the outer cell membrane. (62)

1.5.2 Mechanism of Lp(a) Assembly

Lp(a) assembly is a two step process, in which initial non-covalent association of

apo(a) and apoB is followed by the formation of a covalent bond between the two species (see Figure 1.6). (53) A number of studies have been performed to establish which sequences in apo(a) and apoB are required for Lp(a) assembly. The presence of WLBS in each of KIV_5 to KIV_8 have been demonstrated (52); sequences within KIV_{6-8} appear to be required for non-covalent interaction with apoB. (52,63) This non-covalent interaction of apo(a) and apoB can be inhibited by lysine, lysine analogues, proline, arginine and phenylalanine. (54,64) The WLBS in apo(a) are proposed to be masked in the context of covalent Lp(a) particles. (39,52) Support for this model comes from electron microscopy studies showing that both non-covalent and covalent interactions of apo(a) and apoB are mediated by the C-terminal half of apo(a) (i.e. KIV_{5-10}), while the N-terminus (i.e. N-terminal half) of apo(a) extends out from, and is not directly associated with the Lp(a) particle. (65) The single disulfide bond between apo(a) and apoB in Lp(a) particles has been shown to involve the free cysteine in apo(a) KIV_9 and a cysteine within the C-terminal 50% of apoB. (45,46,66,67,68,69,70)

1.5.3 Animal Models for Lp(a) Assembly

Transgenic mice have been generated that express recombinant human apo(a) [r-apo(a)]. (71,72) In contrast to what is found in humans, the apo(a) was shown to circulate in an uncomplexed free form in the plasma of these mice. No Lp(a) was detected in the transgenic mouse plasma, indicating that human apo(a) and mouse LDL do not associate to form covalent Lp(a) particles. When the mice were injected with a bolus of human LDL, Lp(a) could then be detected in the plasma. (71) Also, double transgenic mice

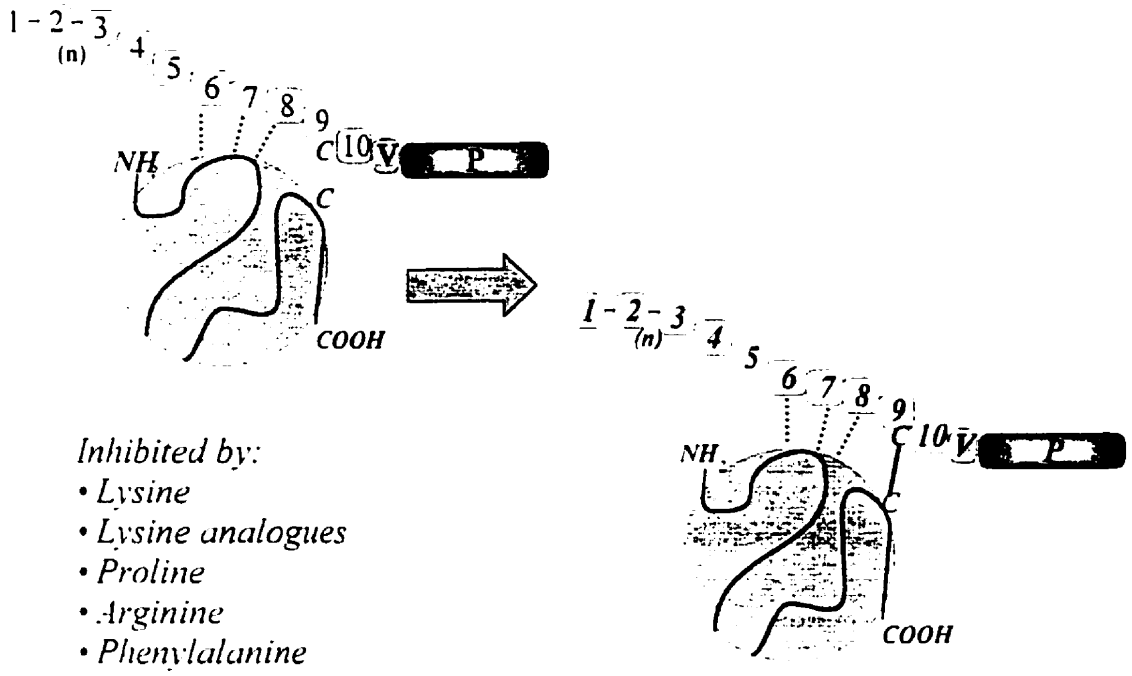

Figure 1.6

Schematic representation of the two step Lp(a) assembly model. Weak lysine binding sites in KIV_{n-3} associate non-covalently with apoB; this association is inhibited upon addition of lysine, lysine analogues, proline, arginine and phenylalanine. In this model, the initial non-covalent association aligns KIV_9 of apo(a) with a free cysteine in apoB (Cys3734). A covalent disulfide bond is formed between the two proteins, completing the second step of Lp(a) assembly.

expressing both human apo(a) and human apoB contained detectable Lp(a) in their plasma. (72) Interestingly, transgenic rabbits expressing human r-apo(a) contain plasma Lp(a) particles composed of human apo(a) and rabbit LDL. (3) This suggests the possibility for comparison between rabbit, mouse and human LDL in helping to understand sequence requirements in apoB for Lp(a) assembly.

1.5.4 Sequence Requirements in ApoB-100 for Lp(a) Formation

The identity of the cysteine of apoB-100 involved in the disulfide bond with apo(a) is somewhat controversial, although it has generally been shown to be located in the C-terminal 50% of apoB. (66,67,68,69,70) Two free cysteines on the surface of LDL have been detected (16), but the exact identity of the cysteine residue in apoB-100 involved in disulfide linkage with apo(a) is unclear. Conflicting evidence points to either the Cys3734 (66,67) or Cys4326 (68,69) of apoB-100 being involved in disulfide linkage to apo(a) to form Lp(a). Due to a combination of evidence generated by fluorescent labeling of apoB100 and computer modeling showing its surface accessibility, Cys3734 has been suggested to be involved in the disulfide linkage with apo(a). (16,67) Several ELISA-based studies [Koschinsky *et al* (66) and Rahman *et al* (74)], have shown that a synthetic apoB fragment corresponding to amino acid sequence 3732-3745 (i.e. spanning Cys3734) binds r-apo(a). Although binding measured is non-covalent and does not directly implicate Cys3734 in disulfide interaction with apo(a), it suggests that surrounding amino acids may mediate initial non-covalent interaction, thus promoting a specific disulfide bond. Contradictory results were found when rat hepatocytes (McA-

Rh7777) were transfected with variably C-terminal truncated apoB species. (70) All truncations analyzed (as large as apoB-94, i.e. containing the amino-terminal 94% of apoB) did not result in covalent association with r-apo(a). Cys3734 is contained within apoB-94, which was interpreted to suggest that Cys4326, which is present within the C-terminal 6% of apoB-100, may be responsible for disulfide linkage to apo(a).

Amino terminal sequences of apoB have been implicated in the initial non-covalent step of Lp(a) assembly. (73) Full length apoB100 and C-terminal truncations of apoB were stably expressed in McA-RH7777 cells. CM from cells expressing the various truncations were then passed over affinity columns consisting of either a 17K r-apo(a) or KIV_{5-8} r-apo(a) immobilized on Sepharose beads; specifically bound protein was considered to be that eluted by the addition of the lysine analogue ε-aminocaproic acid (ε-ACA). It was found that all apoB constructs greater than and including apoB29 bound completely to the apo(a) affinity columns, whereas apoB18 exhibited a decrease in binding affinity and apoB15 did not bind to either column. These results indicate that sequences within the amino terminus of apoB (between the amino terminal 15%-18% of the molecule, corresponding to amino acids 680 to 781) play an essential role in non-covalent interaction with apo(a).

1.5.5 Sequence Requirements in Apo(a) for Lp(a) Formation

A number of studies support the model from electron microscopy studies which showed that the C-terminal half of apo(a) mediates both the non-covalent and covalent interactions with apoB. (65) The apo(a) cysteine residue involved in disulfide linkage to

apoB has been identified by site-directed mutagenesis as Cys4057, the seventh unpaired cysteine in KIV_9 (see Section 1.4). (45,46)

The electron microscopy studies (65) are also consistent with a role for kringles containing WLBS of apo(a) in the initial non-covalent association with apoB-100. Studies using COS cells (from African green monkey *C. aethiops* kidney) transfected with a series of truncated apo(a) derivatives showed that the presence of the KIV_6 was required for efficient Lp(a) assembly. (75) This study also demonstrated that the spacing or distance between KIV_6 and KIV_9 was important, with a required length corresponding to two KIV sequences. The importance of initial non-covalent interactions between WLBS of apo(a) and apoB was further shown by studies using baboon hepatocytes. (60) The accumulation of Lp(a) was observed in the culture medium of the hepatocytes. The addition of the lysine analog 6-AHA caused an inhibition of Lp(a) assembly, providing further evidence that the LBS are required for efficient assembly. Additional studies have been performed by Trieu and McConathy utilizing Chinese Hamster Ovary (CHO) cells transfected with truncated apo(a) derivatives. (53) They showed that a C-terminal derivative of apo(a) containing apo(a) KIV_9 and KIV_{10} followed by the KV and protease-like domains cannot bind to apoB. Inclusion of N-terminal sequences indicated that KIV_6, and possibly KIV-, are required for the initial non-covalent interaction of apo(a) and apoB-100. Reducing the number of KIV_2 sequences from 28 to 17 did not affect the non-covalent interaction of apo(a) and LDL. (53) This seems to contradict the inverse correlation between apo(a) size and Lp(a) concentration in plasma, thus suggesting a possible role for KIV_2 sequences in apo(a) secretion efficiency. (6,22)

Our lab has also examined non-covalent Lp(a) assembly using a variety of N– and C-terminal truncations of apo(a) for binding studies. (66,76) Results demonstrate that removal of KIV_2 domains increases Lp(a) assembly efficiency; the 12K r-apo(a) derivative (containing three KIV_2 domains) bound non-covalently to immobilized LDL with a slightly greater affinity than the 17K r-apo(a) derivative (containing eight KIV_2 domains) (12K K_d=340 nM *vs* 17K K_d=530 nM). This contradicts work by Trieu and McConathy (53) which suggested no role for the number of KIV_2 domains in Lp(a) assembly. This suggests that a critical number of KIV_2 domains can affect Lp(a) assembly. Additional KIV_2 domains above this critical number may cause structural constraints for apo(a)-apoB association, thereby impeding Lp(a) assembly. This also seems to suggest that the inverse relationship between apo(a) size and plasma Lp(a) levels may reflect, at least in part, the efficiency of Lp(a) formation, particularly for very small apo(a) isoform sizes. Results from our lab (66,76) suggest that the WLBS in KIV_5 does not play a significant role in the non-covalent association of apo(a) and apoB-100, since comparison of K_d values between the $KIV_{6\text{-}P}$ derivative (lacking KIV_5, K_d=1800 nM) and the 6K derivative (containing a KIV_1/KIV_5 hybrid, K_d=670 nM) shows that removal of KIV_5 actually increases apo(a) affinity for immobilized LDL. In theses studies, sequential removal of WLBS-containing kringles resulted in a decrease in non-covalent binding affinities to immobilized LDL ($KIV_{6\text{-}P}$, K_d=670 nM; $KIV_{7\text{-}P}$, K_d=1800 nM; $KIV_{8\text{-}P}$, K_d=5100 nM) with no binding detected upon removal of KIV_8. C-terminal deletions of the 6K construct from the protease domain to KIV_9, with WLBs remaining, also exhibited decreases in binding affinities, but never a complete loss of binding (6K, K_d=670 nM;

6KΔVP, K_d=1600 nM; KIV_{5-9}, K_d=2000 nM; KIV_{5-8}, K_d=7900 nM). Comparison of the binding affinities for KIV_{5-8} and KIV_{5-9} contradicts the lack of a role for KIV_9 in non-covalent binding to apoB-100. Also, additional studies in our lab using a purified KIV_9 domain expressed in *E. coli* showed the ability of this kringle to bind, albeit weakly, to immobilized LDL. (74) This interaction was inhibited by lysine, arginine and phenylalanine. These results suggest that the KIV_9 can play a small role in non-covalent binding to apoB-100. Also, site-directed mutagenesis of a key lysine binding site residue in KIV_{10}, Trp72→Arg72, in the context of 17K recombinant apo(a) [r-apo(a)] did not affect non-covalent Lp(a) apo(a)-apoB-100 interaction. (31) This suggests that the lysine binding function of KIV_{10} is not required for Lp(a) assembly. Analysis of a construct encoding apo(a) KIV_{6-8} resulted in the observation of increased non-covalent binding affinity compared to a derivative containing KIV_5 (KIV_{5-8}, K_d=7900 nM; KIV_{6-8}, K_d=4100 nM). (73) Again, this supports previous results that the removal of KIV_5 increases apo(a) affinity for immobilized LDL, suggesting that apo(a) KIV_{6-8} mediates the non-covalent association of apo(a) and apoB-100. (66,76) Also, non-covalent apo(a)-apoB interactions using both the 17K and the KIV_{6-8} derivatives were shown to be inhibited by the addition of arginine, phenylalanine, proline, lysine and lysine analogues. The results suggest that these amino acids can interact with apo(a) through WLBS present in KIV_6, KIV_7, and/or KIV_8, thus disrupting initial non-covalent interactions between apo(a) and apoB. This is consistent with studies by Kostner *et al* (77) demonstrating an initial role for KIV_6 and KIV_7 in the initial non-covalent interaction of apo(a) and apoB-100.

In an additional study, Gabel *et al.* (54) generated stably-transfected human embryonic kidney (293) cells expressing a battery of truncated recombinant apo(a) derivatives, all of which contained the KIV_9 sequence required for covalent Lp(a) formation. Analysis of the initial rate at which successive apo(a) N-terminal truncations formed covalent Lp(a) particles over the first two hours and the maximum efficiency of Lp(a) formation was determined. Comparison of covalent Lp(a) formation of 17K and 12K r-apo(a) derivatives (containing eight and five KIV_2 domains, respectively) showed that removal of KIV_2 kringles results in increased Lp(a) assembly rate (0.9 $nmol \cdot L^{-1} \cdot h^{-1}$ and 1.8 $nmol \cdot L^{-1} \cdot h^{-1}$, respectively) and increased efficiency of formation (~70% and ~89%, respectively). While Trieu and McConathy (53) did not detect an effect of reducing KIV_2 number (from 28 to 17) on Lp(a) assembly, Gabel *et al.* (54) observed an effect by reducing the number of KIV_2 sequences (from eight to five). This suggests that a KIV_2 number greater than eight has no further effect on Lp(a) assembly. The N-terminal truncation, 6-P (encoding a C-terminal sequence of apo(a) from KIV_6 to the protease-like domain), showed an increase in rate (4.3 $nmol \cdot L^{-1} \cdot h^{-1}$) and the same efficiency of formation (~80%) when compared to the 6K (encoding an N-terminal KIV_1/KIV_5 hybrid in addition to the 6-P sequence) rate (3.1 $nmol \cdot L^{-1} \cdot h^{-1}$) and efficiency of formation (~80%). The N-terminal truncation 7-P (encoding a C-terminal sequence of apo(a) from KIV_7 to the protease-like domain) showed a similar rate (3.7. $nmol \cdot L^{-1} \cdot h^{-1}$) and efficiency of formation (~80%) when compared to 6K, but the rate of formation was slightly decreased compared to the previous truncation 6-P. This suggests that KIV_6 plays a role in the initial non-covalent interaction of Lp(a) assembly. Further N-terminal deletions, 8-P and

9-P (encoding C-terminal sequences of apo(a) from KIV_8 to the protease-like domain and from KIV_9 to the protease-like domain, respectively) showed an even more drastic decrease in rate (1.63 $nmol \cdot L^{-1} \cdot h^{-1}$ and 0.3 $nmol \cdot L^{-1} \cdot h^{-1}$, respectively) and efficiency (~57% and ~22%, respectively) of Lp(a) formation, comparing 9-P to 8-P and comparing both to the 7-P truncation. Also, when the KIV_{5-9} derivative was used to form r-Lp(a) particles this Lp(a) was unable to bind to lysine-Sepharose, suggesting that the WLBS are "masked" in the context of Lp(a) and that the strong LBS in KIV_{10} mediates lysine-dependent binding of Lp(a) to biological substrates. Taken together, these data suggest that WLBS in KIV_6, KIV_7, and KIV_8, as well as sequences in KIV_9 are responsible for the initial non-covalent binding of apo(a) and apoB in Lp(a) assembly. These studies are limited in their physiological relevance due to the use of truncated derivatives of apo(a), which could affect apo(a) conformation. As such, abolishment of WLBS in the context of physiological relevant apo(a) derivatives would be more useful.

1.6 Objectives and Hypothesis

The goal of the present study is to further analyze the mechanism of Lp(a) assembly and specifically the role of apo(a) WLBS in this process. Apo(a) derivatives have been generated in which WLBS in KIV types 6-8 have been mutated either singly or in combination. These mutants have been generated in the context of the 17K derivative, which corresponds to a physiologically-relevant apo(a) isoform both in terms of size and kringle composition. These derivatives were then utilized to study both non-covalent and covalent Lp(a) formation.

We hypothesize that disruption of these WLBS will cause a decreased affinity of apo(a) for the apoB component of LDL, resulting in a decrease in both non-covalent and covalent association between these two molecules.

Materials and Methods

2.1 Construction of Plasmids Encoding 17-kringle Recombinant Apolipoprotein(a) Mutant Derivatives

Experiments were performed utilizing 17 kringle (17K) r-apo(a) species (wild-type and mutant derivatives). Sequences encoding the wild-type 17K r-apo(a) were assembled in the pRK5 expression plasmid (78) as previously described (pRK5ha17 plasmid). (38) Construction of 17K derivatives containing point mutations, resulting in the substitution of Glu56→Gly56 (see Figure 2.1) in the weak lysine binding sites (WLBS) in apo(a) KIV_6, KIV_7, and KIV_8 was performed as described below (see Figure 2.2). These mutations cause the disruption of the WLBS and result in decreased binding to lysine-Sepharose columns. (51; W. Sangrar, unpublished data; B. Gabel, unpublished data)

2.1.1 Construction of an Expression Plasmid Encoding the 17KΔWLBS6 Derivative

The plasmid encoding the 6K r-apo(a) derivative (pRK5ha6 plasmid) (54) was used as a PCR template in the construction of an expression plasmid encoding the 17KΔWLBS6 derivative. Primers 1 and 2 (see Table 2.1) were used to produce a 695 bp PCR product (product 1) which was cloned into *Eco*RV-digested pBluescript SK^-. Primers 3 and 4 (see Table 2.1) were used to produce a 505 bp PCR product (product 2) which was cloned into *Eco*RV-digested pBluescript SK^-; fragments in pBluescript were verified by DNAsequence analysis. A 636 bp restriction fragment (generated by digestion

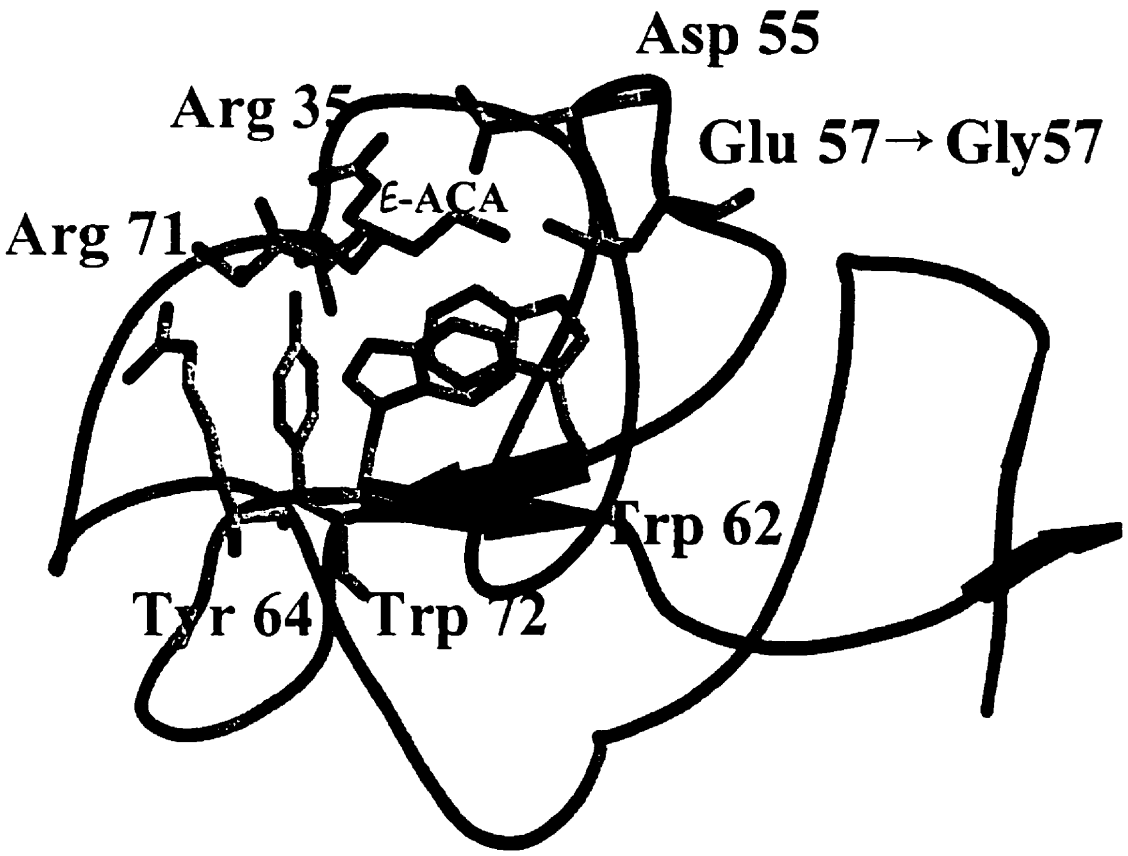

Figure 2.1

Ribbon diagram of KIV_2 showing the position of the mutation (Glu57→Gly57) in the weak lysine binding site; the mutation was introduced in analogous positions in KIV_6 and KIV_3. [Model kindly provided by Dr. Zongchoa Jia, Department of Biochemistry, Queen's University, Kingston, Ontario]

of product 1 with *Eco*RI and *Ngo*MIV) and a 499 bp restriction fragment (generated by digestion of product 2 with *Ngo*MIV and *Eco*RI) were used for a 3-part ligation into *Eco*RI-digested pBluescript. The resulting clone was digested with *Eco*RI/*Aat*II to produce a 730 bp fragment containing the WLBS mutation. The pRK5ha6 plasmid digested together with *Aat*II/*Sal*I, together with the 730 bp *Eco*RI/*Aat*II fragment were used for a three-part ligation into the wild-type pRK5 expression plasmid that had been digested with *Eco*RI/*Sal*I; the resulting plasmid was designated pRK5ha6ΔWLBS6. This plasmid was digested with *Eco*RV/*Sma*I to produce a 1896 bp fragment which then ligated into the pRK5ha17 plasmid digested with *Eco*RV/*Sma*I; a 342 bp *Sma*I fragment (encoding KIV_5) was ligated into this *Sma*I-digested plasmid to give the final expression plasmid designated pK5ha17ΔWLBS6.

2.1.2 Construction of an Expression Plasmid Encoding the 17KΔWLBS7 Derivative

The pRK5ha6 plasmid was used as a PCR template in the construction of an expression plasmid encoding the 17KΔWLBS7 derivative. Primers 5 and 6 (see Table 2.1) were used to produce a 229 bp PCR product (product 3) which was cloned into *Eco*RV-digested pBluescript SK⁻. Primers 7 and 4 (see Table 2.1) were used to produce a 184 bp PCR product (product 4) which was cloned into *Eco*RV-digested pBluescript SK⁻; fragments in pBluescript were verified by DNA sequence analysis. A 233 bp restriction fragment (generated by digestion of product 3 with *Eco*RI and *Ngo*MIV) and a 192 bp restriction fragment (generated by digestion of product 4 with *Ngo*MIV and *Eco*RI) were used for a 3-part ligation into *Eco*RI-digested pBluescript. The resulting

clone was digested with *Eco*RI/*Aat*II to produce a 417 bp fragment containing the WLBS mutation. The pRK5ha6 plasmid digested to produce a 730 bp *Eco*RI/AatII fragment, together with the 417 bp *Eco*RI/*Aat*II fragment were used for a three-part ligation into *Eco*RI-digested pBluescript SK⁻. The resulting clone was digested with *Eco*RI/*Hga*I to produce a 1013 bp fragment containing the WLBS mutation. The pRK5ha6 plasmid digested with *Hga*I/*Bal*I to produce a 816 bp fragment together with the 1013 bp *Eco*RI/*Hga*I fragment were used for a three-part ligation into a pRK5ha6 plasmid lacking sequences encoding the KV and protease domains (pRK5ha6ΔVP) (54) digested with *Eco*RI/*Bal*I. The resulting clone was digested with *Avr*II and a 1678 bp *Avr*II fragment from the pRK5ha6 plasmid (encoding the protease domain) was cloned into the vector; the resulting plasmid was designated pRK5ha6ΔWLBS7. This plasmid was digested with *Eco*RV/*Sma*I to produce a 1896 bp fragment which then ligated into the pRK5ha17 plasmid digested with *Eco*RV/*Sma*I; a 342 bp *Sma*I fragment (encoding KIV_5) was ligated into this *Sma*I-digested plasmid to give the final expression plasmid designated pK5ha17ΔWLBS7.

2.1.3 Construction of an Expression Plasmid Encoding the 17KΔWLBS8 Derivative

The pRK5haKIV$_{6-8}$ plasmid (79) was used as the first PCR template in the construction of an expression plasmid encoding the 17KΔWLBS8 derivative. Primers 1 and 6 (see Table 2.1) were used to produce a 1026 bp PCR product (product 5) which was cloned into *Eco*RV-digested pBluescript SK⁻. The pRK5haKIV$_{3-P}$ plasmid (54) was used as the second PCR template in the construction of an expression plasmid encoding the

17KΔWLBS8 derivative. Primers 8 and 9 (see Table 2.1) were used to produce a 1973 bp PCR product (product 6) which was cloned into *Eco*RV-digested pBluescript SK$^-$; fragments in pBluescript were verified by DNA sequence analysis. A 787 bp restriction fragment (generated by digestion of product 5 with *Eco*RI and *Ngo*MIV) and a 1972 bp restriction fragment (generated by digestion of product 6 with *Ngo*MIV and *Eco*RI) were used for a 3-part ligation into *Eco*RI-digested pBluescript. The resulting clone contained a 404 bp *Eco*RI/*Aat*II fragment (upstream from the WLBS mutation) which was removed and replaced with a 730 bp *Eco*RI/*Aat*II fragment (see Section 2.1.2) from the pRK5ha6 plasmid. The resulting clone was digested with *Bal*I to produce a 1796 bp fragment containing the WLBS mutation; this fragment was ligated into the pRK5ha6ΔVP plasmid which had been digested with *Bal*I. The resulting clone contained a 580 bp *Avr*II fragment which was removed and replaced with a 1678 bp *Avr*II fragment from the pRK5ha6 plasmid (encoding the protease domain); the resulting plasmid was designated pRK5ha6ΔWLBS8. This plasmid was digested with *Eco*RV/*Sma*I to produce a 1896 bp fragment which then ligated into the pRK5ha17 plasmid digested with *Eco*RV/*Sma*I; a 342 bp *Sma*I fragment (encoding KIV_5) was ligated into this *Sma*I-digested plasmid to give the final expression plasmid designated pK5ha17ΔWLBS8.

2.1.4 Construction of an Expression Plasmid Encoding the 17KΔWLBS6.7 Derivative

The pRK5ha6ΔWLBS6 plasmid (see Section 2.1.1) was digested with *Eco*RI/*Aat*II to produce a 730 bp fragment (encoding for the KIV_5 and KIV_6 domains). The pRK5ha6ΔWLBS7 plasmid (see Section 2.1.2) was digested with *Aat*II/*Eco*RV to

produce a 1621 bp fragment. The 730 bp restriction fragment and the 1621 bp restriction fragment were used for a 3-part ligation into *Eco*RI/*Eco*RV-digested pRKha6 plasmid; the resulting plasmid was designated pRK5ha6ΔWLBS6,7. This plasmid was digested with *Eco*RV/*Sma*I to produce a 1896 bp fragment which then ligated into the pRK5ha17 plasmid digested with *Eco*RV/*Sma*I; a 342 bp *Sma*I fragment (encoding KIV_5) was ligated into this *Sma*I-digested plasmid to give the final expression plasmid designated pK5ha17ΔWLBS6,7.

2.1.5 Construction of an Expression Plasmid Encoding the 17KΔWLBS7,8 Derivative

The pRK5ha6 plasmid was linearized with *Ngo*MIV. The linearized plasmid was then blunt-ended with Mung Bean Nuclease (MBN; NEB) and re-ligated, resulting in the removal of the *Ngo*MIV site, designated pRK5ha6Δ*Ngo*MIV. The pRK5ha6ΔWLBS7 plasmid (see Section 2.1.2) was digested with *Eco*RI/*Ngo*MIV producing a 954 bp fragment. The pRK5ha6ΔWLBS8 plasmid (see Section 2.1.3) was digested with *Ngo*MIV/*Sal*I producing a 1906 bp fragment. The 954 bp restriction fragment and the 1906 bp restriction fragment were used for a 3-part ligation into the pRK5ha6Δ*Ngo*MIV plasmid that had been digested with *Eco*RI/*Sal*I; the resulting plasmid was designated pRK5ha6ΔWLBS7,8Δ*Ngo*MIV. The pRK5ha6ΔWLBS7 plasmid (see Section 2.1.2) was used as a PCR template in a subsequent step in the construction of an expression plasmid encoding the 17KΔWLBS7,8 derivative. Primers 5 and 6 (see Table 2.1) were used to produce a 571 bp PCR product (product 7) which was cloned into *Eco*RV-digested pBluescript SK^-; the fragment in pBluescript was verified by DNA sequence analysis. A

342 bp restriction fragment (generated by digestion of product 7 with *Ngo*MIV) was ligated into the pRK5ha6ΔWLBS7,8Δ*Ngo*MIV plasmid that had been digested with *Ngo*MIV; the resulting plasmid was designated pRK5ha6ΔWLBS7,8. This plasmid was digested with *Eco*RV/*Sma*I to produce a 1896 bp fragment which then ligated into the pRK5ha17 plasmid digested with *Eco*RV/*Sma*I; a 342 bp *Sma*I fragment (encoding KIV_5) was ligated into this *Sma*I-digested plasmid to give the final expression plasmid designated pK5ha17ΔWLBS7,8.

Primer #	Sequence
1	CCACAGGTGTCCACTCCC
2	AGGACTAAT**GCCGGC**ATCTGGATTCCT
3	AATCCAGAT**GCCGGC**ATTAGTCCTTGG
4	CCTGGACCCCAGTGCTGTTT
5	GTCCACGGCTGTTTCTGAACAA
6	GCGAAT**GCCGGC**ATCTGGATTCCT
7	CCAGAT**GCCGGC**ATTCGCCCTTGGTGTTAT
8	CCAGAT**GCCGGC**ATTCGCCCTTGGTGTTAC
9	TAACCATTATAAGCTGC

Table 2.1

Table of primers used for PCR amplification in the construction of the 17KΔWLBS derivatives. Restriction sites are underlined, while mutated residues are in bold.

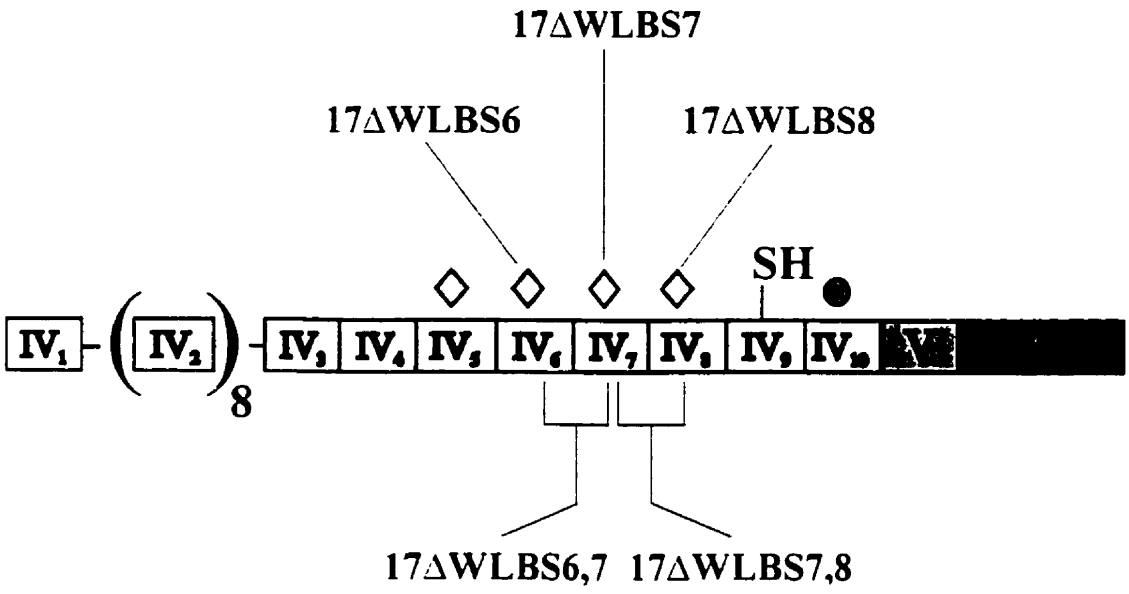

Figure 2.2

Identification of WLBS mutations in the 17K r-apo(a). Apo(a) contains ten types of kringle IV (KIV) sequences (KIV_1- KIV_{10}) followed by a single copy of the kringle V (KV) and protease-like (P) domains. This is a schematic of the 17 kringle r-apo(a) which contains eight copies of the KIV_2 sequence, and corresponds to a naturally-occurring apo(a) isoform. Diamonds indicate weak lysine binding sites (WLBS) present in each of the KIV_5, KIV_6, KIV_7, and KIV_8 with site-directed mutants labeled accordingly. The circle represents a strong lysine binding site present in apo(a) KIV_{10}.

2.2 Isolation of 17K r-apo(a) Apolipoprotein(a) and Mutant Derivatives

2.2.1 Transfection and Expression of 17K r-apo(a) Wild-Type and Mutant Derivatives

Human embryonic kidney (293) cells were routinely cultured at 37°C in Minimal Essential Medium (MEM; Gibco/BRL) supplemented with 5% Fetal Calf Serum (FCS; ICN). Cell lines expressing 17K r-apo(a) (wild-type and derivatives) were generated by transfection of 293 cells by the calcium phosphate co-precipitation method. (80) Transient transfections of 293 cells expressing r-apo(a) derivatives, used in covalent assembly assays (see Section 2.4.3), were generated by transfection with 10 μg of expression plasmid per 100 mm plate. Transiently transfected cells were rescued 5 hours post-transfection by washing with phosphate buffered saline (PBS) and incubated at 37°C in OptiMEM (Gibco/BRL; 6 ml/100mm plate) for 48 hr. At this time, the conditioned media (CM) was harvested and clarified by brief centrifugation (Beckman H-20, 4000 rpm for 5 min). Levels of apo(a) in the CM were determined by Enzyme-linked Immunosorbant Assay (ELISA) (see Section 2.2.2) and the CM was stored at -20°C prior to use. Cells stably expressing r-apo(a) derivatives, which were used for non-covalent binding assays (see Section 2.4.2), were generated by calcium phosphate co-precipitation (80) with 10 μg of expression plasmid and 1 μg of a plasmid encoding the neomycin resistance gene (81) per 100 mm plate. Stably-transfected cells were rescued 5 hr post-transfection by washing with PBS and then incubated at 37°C in serum-containing MEM. Stably-transfected cells were selected by culturing cells in the presence of the selective agent Geneticin (G418; Gibco/BRL; 800 μg/ml of media). After several weeks, G418-

resistant foci were removed from the 100 mm plates and transferred to 24-well plates. Levels of expression were determined by ELISA (see Section 2.2.2). Cells expressing the highest levels of apo(a) were then transferred to 100 mm plates. Dilution cloning of each line was then performed to obtain clonal populations. Stably-expressing lines were used to seed roller bottles (Corning). Cells were allowed to adhere to roller bottles for a 48 hr period, at which time MEM was replaced with OptiMEM for subsequent harvests. CM was collected every three days for approximately one month; media was clarified by brief centrifugation (Beckman J-6B, 3000 rpm for 5 min) and stored at -20°C.

2.2.2 *Determination of Apolipoprotein(a) Concentration by Enzyme-linked Immunosorbant Assay (ELISA)*

The sheep polyclonal capture antibody, AB5-33A [raised against 17K r-apo(a)], was immobilized in microtiter wells [10 µg/ml in coating buffer (50 mM $NaHCO_3$, pH 9.6; 100 µl/well)] overnight at 4°C. The wells were washed four times with 150 µl/well PBS-Tween (PBST; PBS containing 0.1% Tween-20). The wells were then incubated with 150 µl/well blocking buffer (PBS containing 0.2% BSA) at 4°C for 2 hr, to block non-specific binding sites. Wells were then washed four times with PBST. The purified 17K r-apo(a) wild-type derivative was used as a standard for the assay (0 pM to 20 pM in HBS containing 1% BSA and 0.1% Tween-20). CM from transfections (stable or transient transfections, as described in Section 2.2.1) were diluted 1:100 in diluent buffer to produce the stock concentration; 1/2 dilution of the stock, followed by subsequent of 1/2 dilutions in diluent buffer were performed. The wells were incubated with 100

µl/well of each r-apo(a) derivative media at 4°C for 2 hr. Wells were then washed four times with PBST. The wells were then incubated with 100 µl/well of a 1:3000 dilution of the primary antibody in diluent buffer at room temperature for 2 hr. The primary antibody was the monoclonal antibody, Mab-34, that is specific to the protease-like domain of apo(a). After incubation with the primary antibody the wells were washed four times with PBST. The wells were then incubated with 100 µl/well of a 1:3000 dilution of anti-mouse IgG conjugated to horseradish peroxidase at room temperature for 1 hr. The wells were then washed four times with PBST. Detection of secondary antibody binding was performed by addition of 100 µl/well colour development buffer (0.05 M phosphate-citrate buffer, pH 5.0, containing 1 *O*-phenylenediamine tablet, 0.4 mg/ml, and 1.2% H_2O_2). The colour reaction was stopped by the addition of 50 µl/well of 2.0 M H_2SO_4. A TiterTek plate reader was used to measure absorbance readings at 490 nm and 650 nm. Linear regression was performed on readings from the 17K r-apo(a) wild-type derivative standard and concentrations of apo(a) in CM harvests were determined using the standard curve.

2.2.3 Purification of 17K r-apo(a) Wild-Type and Mutant Derivatives

Cultured media from cell lines stably expressing each r-apo(a) derivative was thawed and filtered. A lysine-Sepharose CL-4B (Pharmacia) column was used for the purification of each r-apo(a) derivative by affinity chromatography, as previously described. (54) Briefly, the column (40 ml) was equilibrated with PBS, pH 7.4 containing 0.5 M NaCl (PBS/NaCl). CM from each stably transfected cell line was

passed over the column. The column was then washed with 10 column volumes of PBS/NaCl to elute non-specifically and weakly-bound proteins. Derivatives of r-apo(a) were then eluted with PBS/NaCl containing 0.2M ε-ACA to elute specifically-bound apo(a) derivatives. Fractions containing protein, as determined by measuring the absorbance at 280 nm, were pooled in dialysis tubing (Fisher) and dialyzed against HEPES Buffered Saline (HBS) (four changes of 4L each). Polyethyleneglycol (Fluka) with a molecular weight cut-off of 20 000 (PEG-20 000) was used to concentrate the protein to a desirable volume/concentration. Final protein concentration was determined by measuring absorbance at 280 nm using an extinction coefficient determined by the tyrosine difference spectral method. (38) Purified proteins were aliquoted and stored at -70°C.

2.2.4 SDS-PAGE Analysis of 17K and Mutant Derivatives Produced by Transient or Stable Expression

The 17K r-apo(a) and mutant derivatives produced by transfection of 293 cells were diluted in 2X Laemmli buffer. (82) Samples were analyzed by SDS-PAGE using 6% polyacrylamide gels. Stably-expressed proteins were visualized by silver-staining, while transiently-expressed proteins were subjected to Western blotting in transfer buffer (25 mM Tris, 192 mM glycine, 10% methanol, pH 8.4). Following transfer, the membrane was incubated in blocking solution (6% Casein in 1X NET; 1.5 M NaCl, 50 mM EDTA 0.5 M Tris, 0.5% Triton X-100, pH 7.4) overnight at room temperature, with constant shaking. The following day, the membrane was incubated with the primary

monoclonal antibody, Mab34, (1:3000 dilution in 1X NET) for 1 hr at room temperature. The membrane was then washed four times, for 15 min each, with 1X NET and incubated with the anti-mouse IgG conjugated to horseradish peroxidase (HRP) (1:3000 dilution in 1X NET) for 1 hr at room temperature. The membrane was again washed four times, for 15 min each, with 1X NET. The blot was developed using a chemiluminescence kit (ECL: Amersham).

2.3 Isolation of LDL from Human Plasma

Whole blood, containing 1 mM EDTA to prevent coagulation, was subjected to low-speed centrifugation (Beckman J-6B) at 710g for 20 min at room temperature in order to isolate plasma. The plasma, supplemented with 1mM phenylmethylsulfonylfluoride (PMSF) was used to isolate LDL by sequential flotation, as previously described. (83) Briefly, the plasma (60 ml) was adjusted to a d=1.02 g/mL using sodium bromide and centrifuged at 30 000 rpm (Beckman, 60 Ti rotor) for 20 hr at 10°C. The top fraction (d<1.02 g/mL) was removed and discarded. The infranatant was supplemented with 1mM EDTA and 1mM PMSF and then adjusted to d=1.063 g/mL using sodium bromide and centrifuged under the same conditions. The top fraction (1.02 g/mL < d < 1.063 g/mL), containing LDL, was removed. This fraction was supplemented with 1mM EDTA and 1mM PMSF, diluted with TE buffer (100mM Tris, pH 7.4, containing 1mM EDTA), and adjusted to d=1.063 g/mL using sodium bromide. This solution was then centrifuged at 30 000 rpm (Beckman, 70.1 Ti rotor) for 20 hr at 10°C. The floating LDL-containing fraction was removed and supplemented with 1mM PMSF.

This fraction was then dialyzed overnight at 4°C against 20 mM HBS, pH 7.4. Protein concentration was determined utilizing a modified Bradford assay (Bio-Rad) (76) with bovine serum albumin (BSA; ICN) as a reference standard. LDL was stored at 4°C and was used within a maximum of five days of isolation. An aliquot of isolated LDL was analyzed by SDS-PAGE (82) using a 6% polyacrylamide gel. The LDL was visualized by Coomassie Blue staining.

2.4 Assays for Non-covalent and Covalent Lp(a) Assembly

2.4.1 Fluorescent Labeling of Isolated LDL

Isolated LDL was fluorescently labeled by incubation with a 50-fold molar excess of iodoacetamidofluorescein (5'-IAF; Pierce) overnight at 4°C in the dark. A diethylaminoethylene anion-exchange column (DEAE; Sigma) was pre-incubated with HBS and the labeled LDL was passed over the column to remove unbound label. Labeled LDL was collected in 500 µL fractions. Protein-containing fractions, as determined by the modified Bradford assay (see Section 2.3) with BSA as a reference standard, were pooled and dialyzed overnight in the dark against HBS containing 0.01% (v/v) Tween-20 (HBST; Sigma). The modified Bradford assay was used to determine final LDL concentration. An aliquot of labeled LDL was analyzed by SDS-PAGE (82) using a 6% polyacrylamide gel. The labeled LDL was visualized by Coomassie Blue staining and under ultra-violet light.

2.4.2 Fluorescence Assays to Determine Non-covalent Apo(a)-LDL Association

The 5'-IAF labeled LDL (Flu-LDL), prepared as described above (see Section 2.4.1), was diluted to a concentration of 50 nM in HBST. The 17K r-apo(a) wild type and mutant derivatives were diluted to 2 μM in 50 nM Flu-LDL. The fluorometer wavelengths were set at λexcitation=490 nm and λemission=535 nm. The slit sizes for the light beam of the fluorometer were set at excitation slit=2.5 nm and emission slit=5 nm with the filter cutoff=515 nm. Titrations were performed at room temperature. For each run, a 400 μl aliquot of 50 nM Flu-LDL was added to the fluorometer cuvette and a baseline reading was obtained over a 10 min period. Increasing concentrations of either the 17K or corresponding derivatives were added to the cuvette and changes in fluorescence readings were recorded. Note that the Flu-LDL in the cuvette was maintained at a constant concentration. Data were fit to Equation 1, describing the relationship between change in fluorescence and binding affinity.

Equation 1:

$$\Delta F = F_0 + 0.5 * dI * (Kd + [P] + [\text{Flu-LDL}] - ((Kd + [P] + [\text{Flu-LDL}])^2 - 4 * [P] * [\text{Flu-LDL}])^{0.5})$$

where ΔF=absolute value of change in fluorescence

F_0=baseline fluorescence reading for 50 nM Flu-LDL

dI=unit of fluorescence change per nM of apo(a) protein as determined by non-linear regression

Kd=binding affinity of apo(a) to Flu-LDL as determined by non-linear regression

[P]=concentration of apo(a) protein at each titration point

[Flu-LDL]=concentration of Flu-LDL throughout titration (50 nM)

2.4.3 Covalent Lp(a) Assembly Time Course

CM harvested from each transient transfection of the17K r-apo(a) wild type and mutant derivatives was diluted to 2 nM final apo(a) concentration in HBS and added to a 25-fold molar excess of isolated LDL. The reactions (1 ml final volume) were then incubated in a 37°C water bath. At the desired time points (0, 0.5, 1, 2, 4, 6, 8, and 24 hr), 100 µL of each reaction mixture was removed and added to an eppendorf tube containing 100 µL of 2X SDS sample buffer. (82) Samples were placed at -20°C immediately. Upon completion of the time course assay, 6% SDS-PAGE (under non-reducing conditions) followed by Western blot analysis was performed as described above (see Section 2.2.4). Two bands were detected, a lower band representing free 17K r-apo(a) wild-type or mutant derivative and a higher molecular weight band containing r-apo(a) covalently associated with LDL to form r-Lp(a). Films were scanned using a ScanJet 3C and densitometric analysis (SigmaGel) was performed. The percentage of Lp(a) particle formed at each time point was determined using Equation 2.

Equation 2:

r-Lp(a) formed (%)=Intensity of r-Lp(a)/(Intensity of free apo(a)+Intensity of r-Lp(a))

Results

3.1 Non-covalent Association of Fluorescently-labeled LDL and 17K r-apo(a) Derivatives

3.1.1 Expression and Purification of 17K r-apo(a) Wild-type and Derivatives

The sequences encoding the wild-type 17K r-apo(a) and mutant constructs were assembled in the pRK5 expression plasmid (78) as previously described (see Section 2.1). (38) Human embryonic kidney (293) cell lines stably expressing 17K r-apo(a) (wild-type and mutant derivatives) were generated by transfection of cells with 10 μg of expression plasmid and 1 μg of a plasmid encoding the neomycin resistance gene per 100 mm plate by the calcium phosphate co-precipitation method (see Section 2.2.1). (80) For the purification of the r-apo(a) derivatives serum-free CM from each stably expressing cell line was chromatographed over a lysine-Sepharose affinity column. (54) The concentrations of purified 17 K r-apo(a) and mutant derivatives were determined by measuring absorbance at 280 nm using an extinction coefficient [MW=278,719, $\varepsilon_{0.1\%}$(280nm)=2.07] determined by the tyrosine difference spectral method. (38) Samples containing 200 ng of each protein were then electrophoresed on a 6 % SDS-PAGE gel, under non-reducing conditions, followed by silver staining. The presence of a single band was observed for each derivative, migrating at a comparable position to that of purified 17K r-apo(a) (see Figure 3.1) Purified proteins were stored at -70°C prior to use.

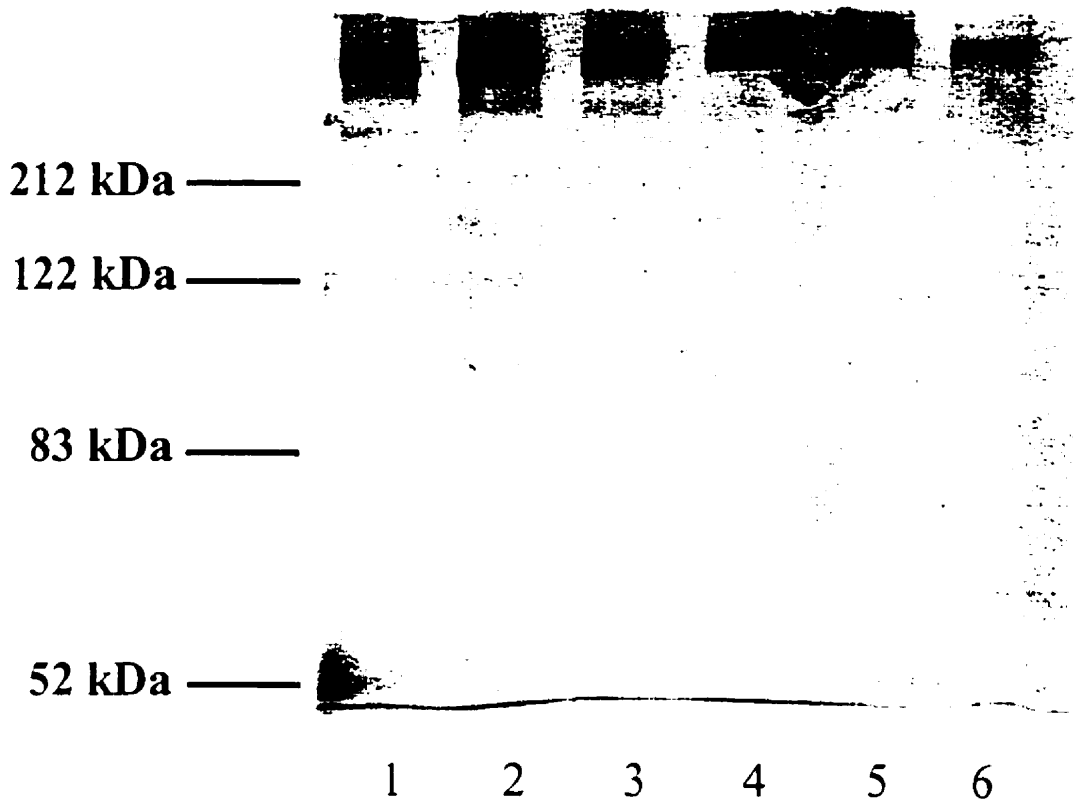

Figure 3.1

Analysis of purity of 17K r-apo(a) proteins (wildtype and mutant derivatives) by SDS-PAGE on a 10% polyacrylamide gel, followed by silver staining. Approximately 200 ng of each protein was loaded per lane. Lane 1: 17K; Lane 2: 17ΔWLBS6; Lane 3: 17ΔWLBS7; Lane 4: 17ΔWLBS8; Lane5: 17ΔWLBS6,7; Lane 6: 17ΔWLBS7,8.

3.1.2 Isolation and Fluorescent Labeling of Human LDL

Fresh-frozen plasma, containing 1 mM EDTA and 1 mM PMSF, was used to isolate LDL by the method of sequential flotation. (83) LDL was fluorescently labeled with iodoacetamidofluorescein and stored at 4°C in the dark. Protein content was determined utilizing a modified Bradford assay (see Section 2.3) with BSA as a reference standard. Concentrations of labeled LDL (Flu-LDL) ranged from ~0.7 mg/ml (1.4 μM) to ~1.2 mg/ml (2.4 μM).

3.1.3 Fluorescent Binding Assays

The Flu-LDL was diluted in HBS, containing 0.1% Tween-20, to a final concentration of 50 nM. The 17K r-apo(a) (wild type and mutant derivatives) were diluted to 2 μM, in 50 nM Flu-LDL containing 0.1% Tween-20. An initial 400 μl aliquot of 50 nM Flu-LDL was added to the fluorometer cuvette and a baseline reading was obtained over a 10 min period. The titration of each 17K r-apo(a) derivative was performed and changes in fluorescence readings were recorded. Average fluorescence readings, for each r-apo(a) concentration, were determined over a two minute interval. These data were subjected to non-linear regression analysis using Equation 1.

Fit curves (see Figures 3.2A, 3.2B, 3.2C, 3.2D, 3.2E, 3.2F, 3.2G) were produced using values obtained from Equation 1. It should be noted that actual binding experiments resulted in a decrease in fluorescence intensity of Flu-LDL. This change was expressed as an absolute value and therefore is shown graphically as a positive change, i.e. percentage change with respect to initial baseline reading. Equation 1 was used to

determine the K_d value, or binding affinity, for each 17K r-apo(a) protein (wild-type and mutant derivatives) with Flu-LDL. In an attempt to address potential variation in LDL preparations the 17K r-apo(a) wild-type was run as a standard for each Flu-LDL preparation. The 17K r-apo(a) mutant binding affinities for Flu-LDL were compared to the 17K r-apo(a) wild-type standard analyzed for binding to the respective Flu-LDL preparation (see Table 3.1). Data shown are representative of experiments performed a minimum of two times.

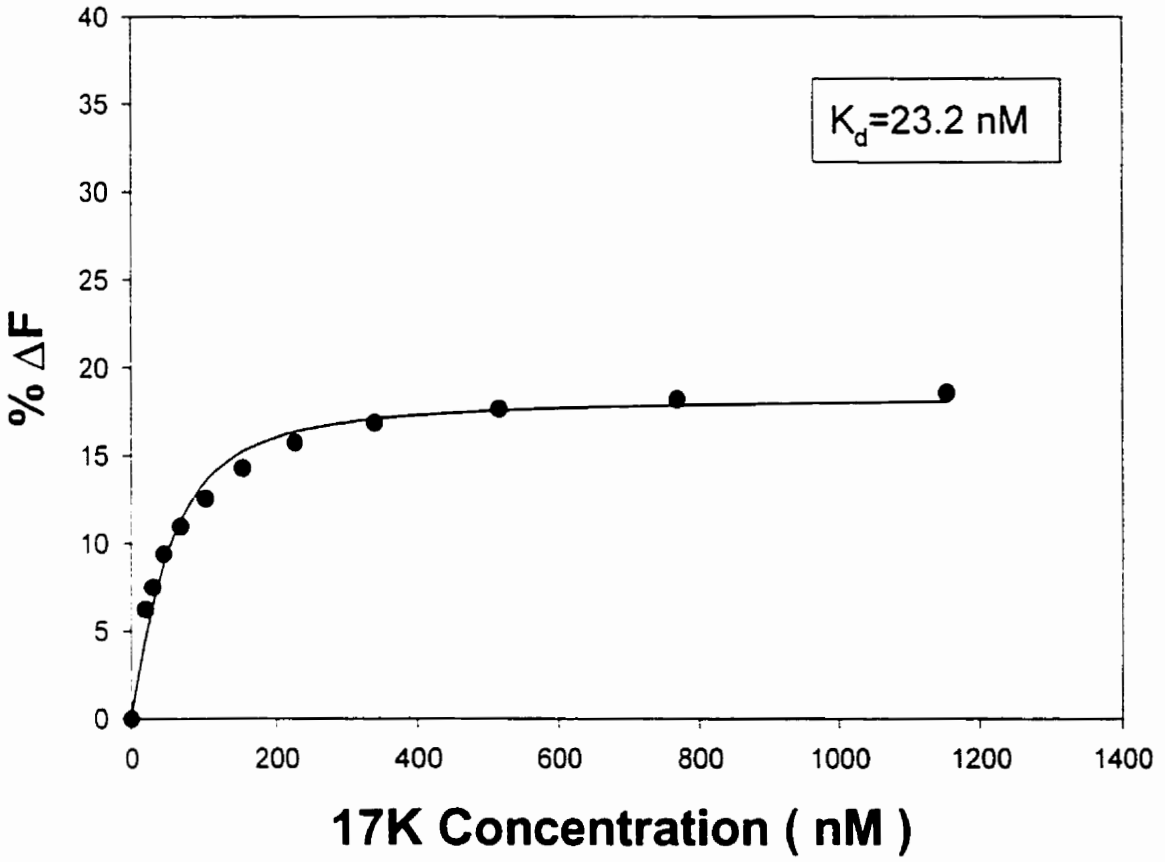

Figure 3.2A

Binding of 17K r-apo(a) to Flu-LDL (50 nM) in solution phase. Circles represent changes in percent fluorescence readings, while the line represents the data fit to Equation 1. The change in fluorescence is expressed as a positive percentage change with respect to the fluorescence reading of Flu-LDL alone. The binding affinity value, K_d, of the 17K for Flu-LDL is included.

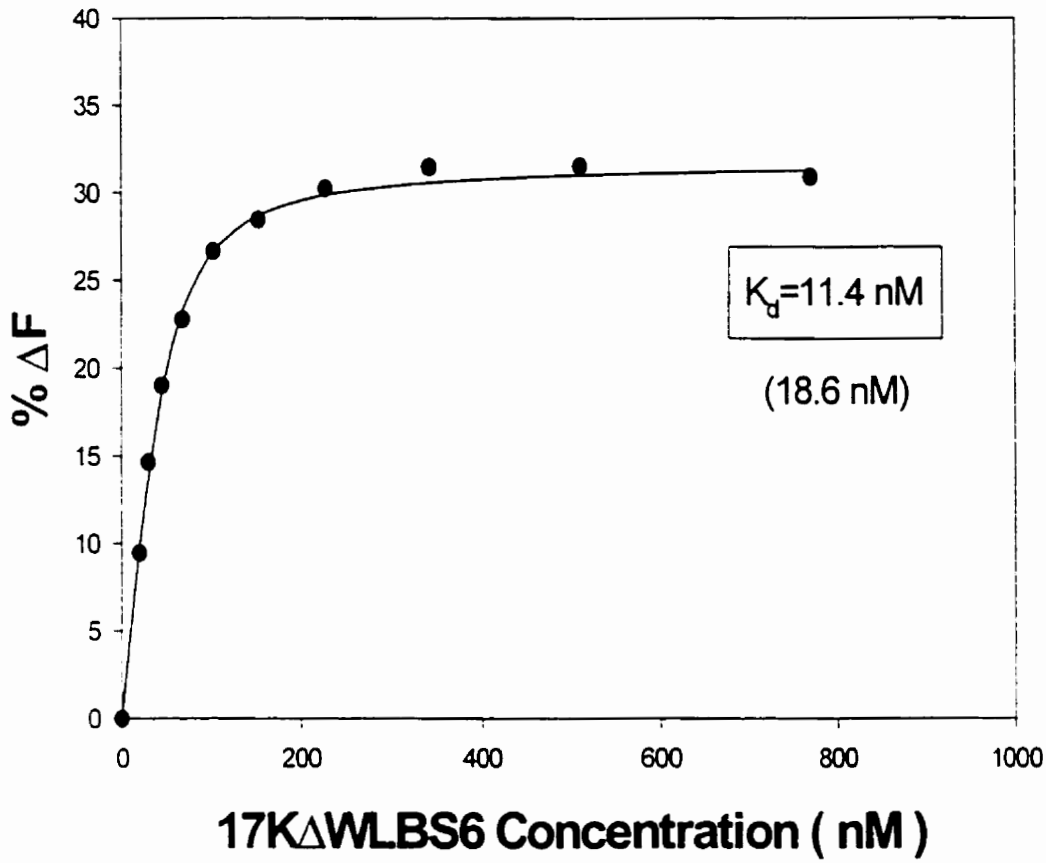

Figure 3.2B

Binding of 17KΔWLBS6 r-apo(a) to Flu-LDL (50 nM) in solution phase. Circles represent changes in percent fluorescence readings, while the line represents the data fit to Equation 1. The change in fluorescence is expressed as a positive percentage change with respect to the fluorescence reading of Flu-LDL alone. The binding affinity value, K_d, of the 17KΔWLBS6 for Flu-LDL is included, along with that of the 17K performed as a control (in brackets).

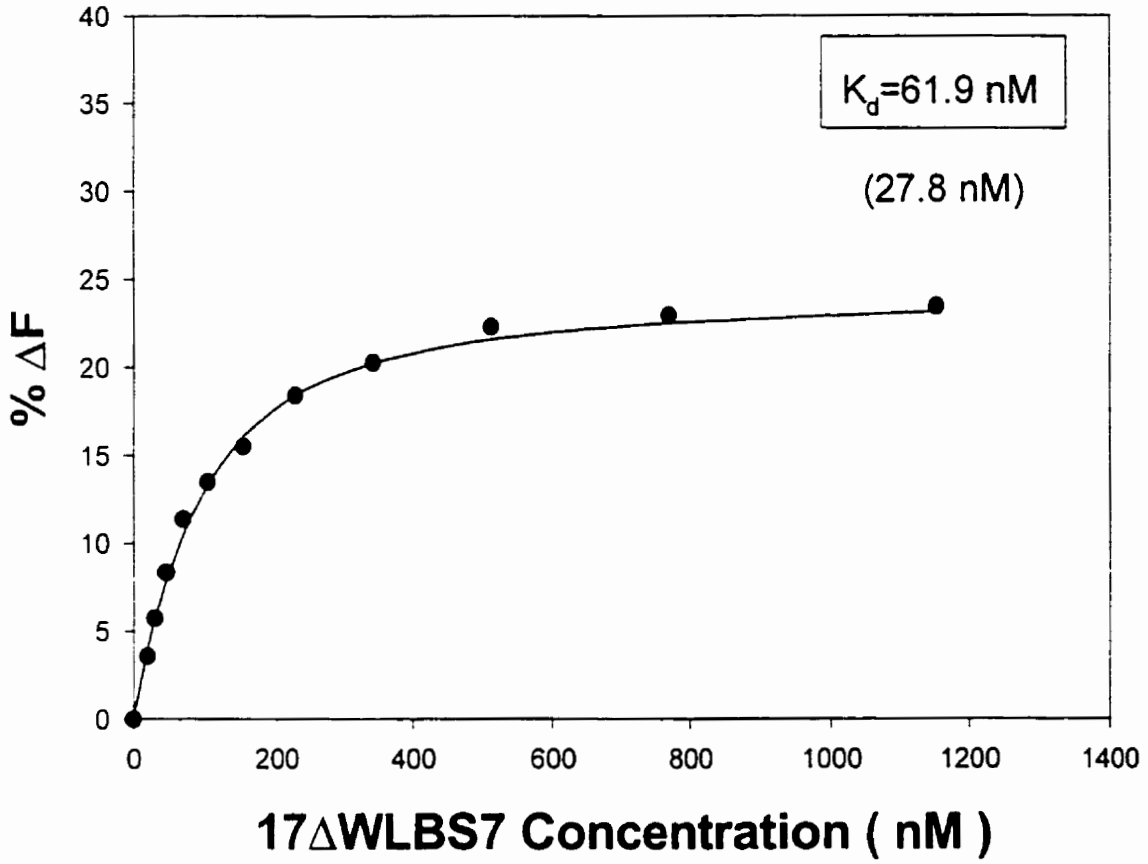

Figure 3.2C

Binding of 17KΔWLBS7 r-apo(a) to Flu-LDL (50 nM) in solution phase. Circles represent changes in percent fluorescence readings, while the line represents the data fit to Equation 1. The change in fluorescence is expressed as a positive percentage change with respect to the fluorescence reading of Flu-LDL alone. The binding affinity value, K_d, of the 17KΔWLBS7 for Flu-LDL is included, along with that of the 17K performed as a control (in brackets).

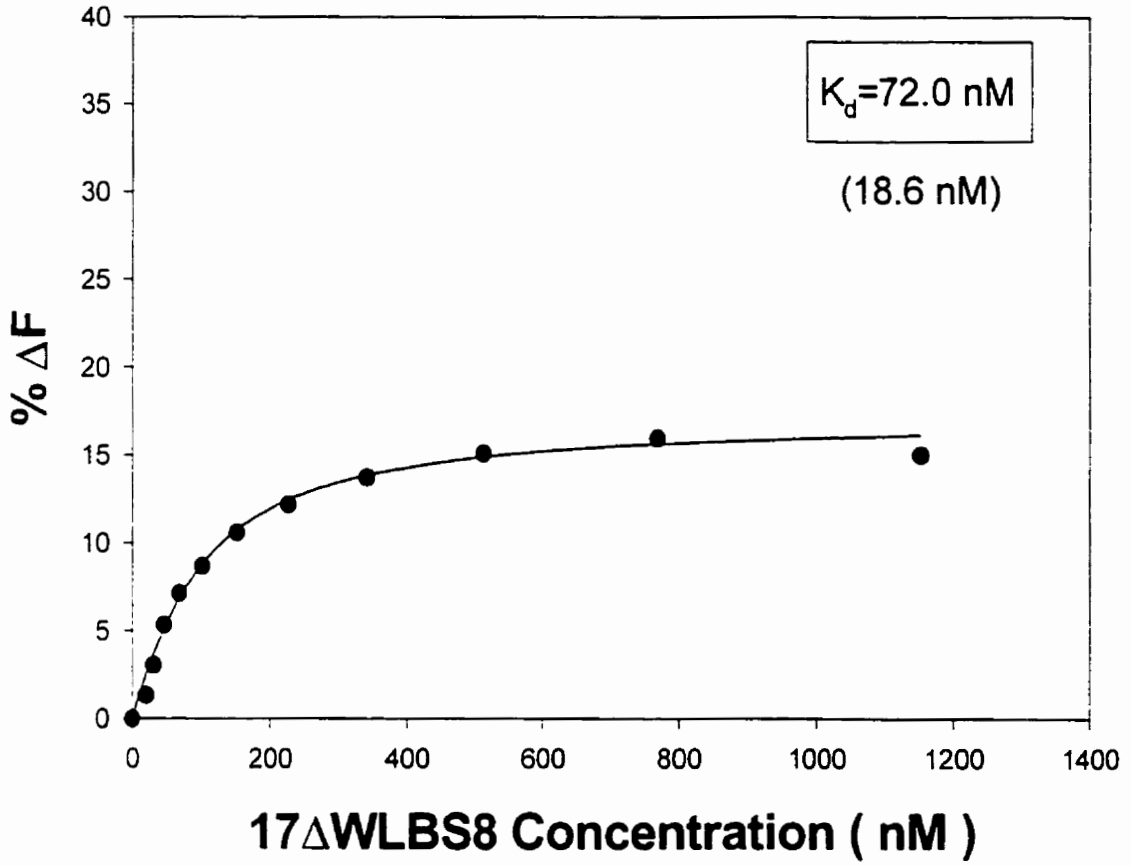

Figure 3.2D

Binding of 17KΔWLBS8 r-apo(a) to Flu-LDL (50 nM) in solution phase. Circles represent changes in percent fluorescence readings, while the line represents the data fit to Equation 1. The change in fluorescence is expressed as a positive percentage change with respect to the fluorescence reading of Flu-LDL alone. The binding affinity value, K_d, of the 17KΔWLBS8 for Flu-LDL is included, along with that of the 17K performed as a control (in brackets).

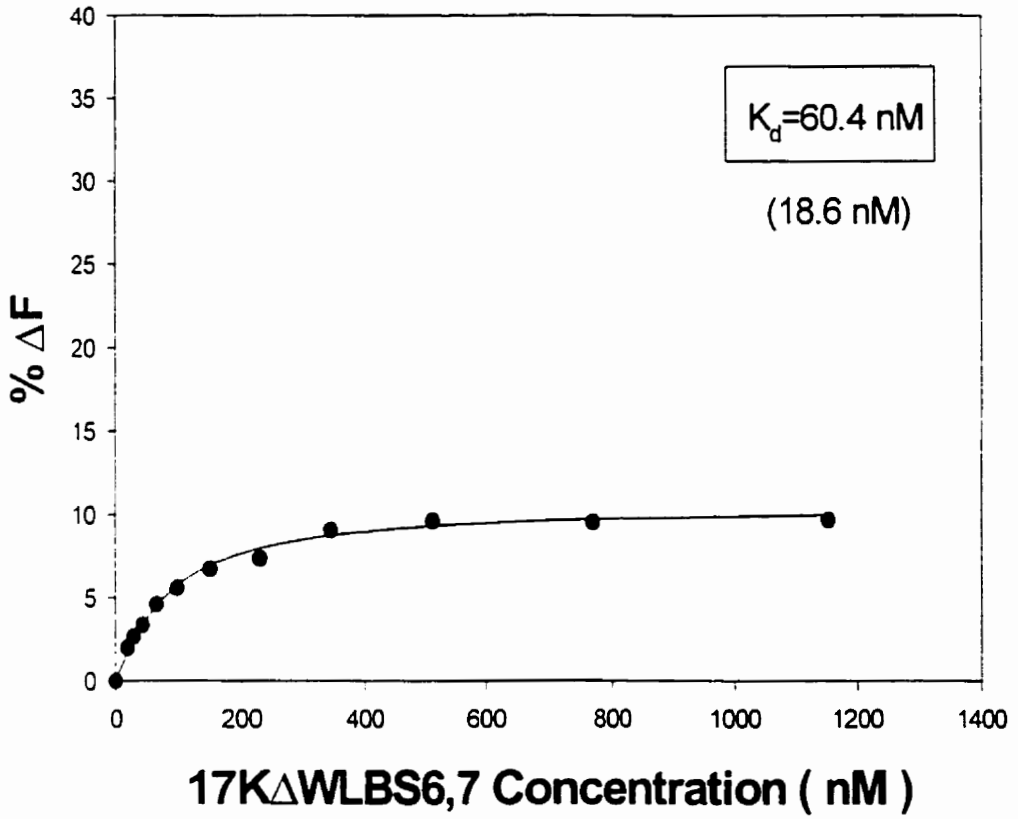

Figure 3.2E

Binding of 17KΔWLBS6,7 r-apo(a) to Flu-LDL (50 nM) in solution phase. Circles represent changes in percent fluorescence readings, while the line represents the data fit to Equation 1. The change in fluorescence is expressed as a positive percentage change with respect to the fluorescence reading of Flu-LDL alone. The binding affinity value, K_d, of the 17KΔWLBS6,7 for Flu-LDL is included, along with that of the 17K performed as a control (in brackets).

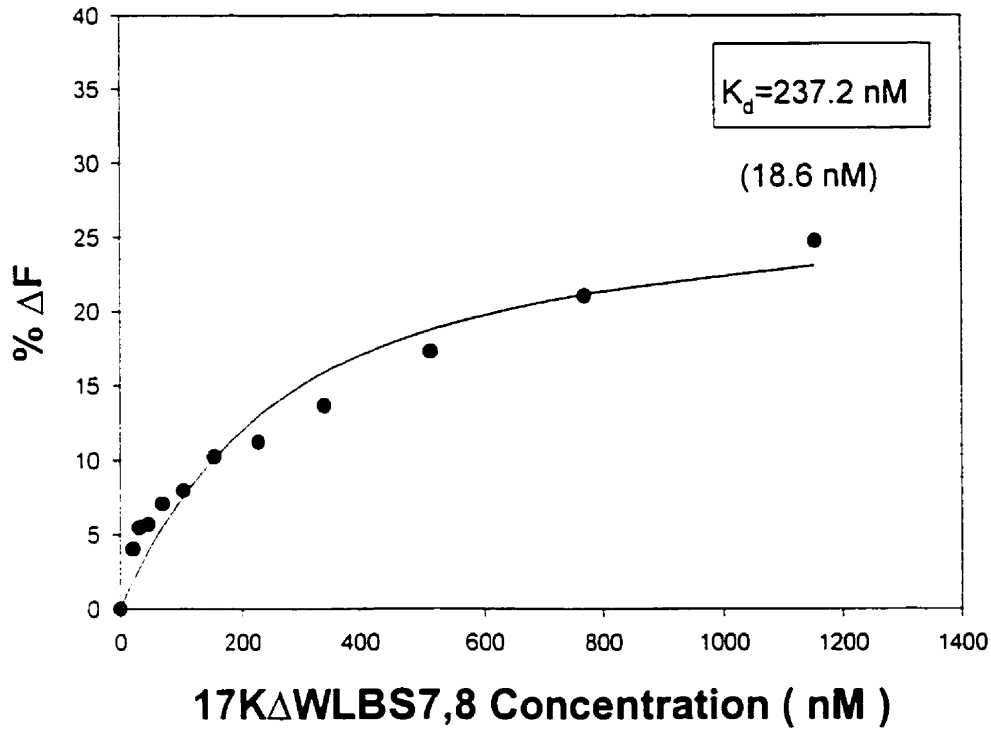

Figure 3.2F

Binding of 17KΔWLBS7,8 r-apo(a) to Flu-LDL (50 nM) in solution phase. Circles represent changes in percent fluorescence readings, while the line represents the data fit to Equation 1. The change in fluorescence is expressed as a positive percentage change with respect to the fluorescence reading of Flu-LDL alone. The binding affinity value, K_d, of the 17KΔWLBS7,8 for Flu-LDL is included, along with that of the 17K performed as a control (in brackets).

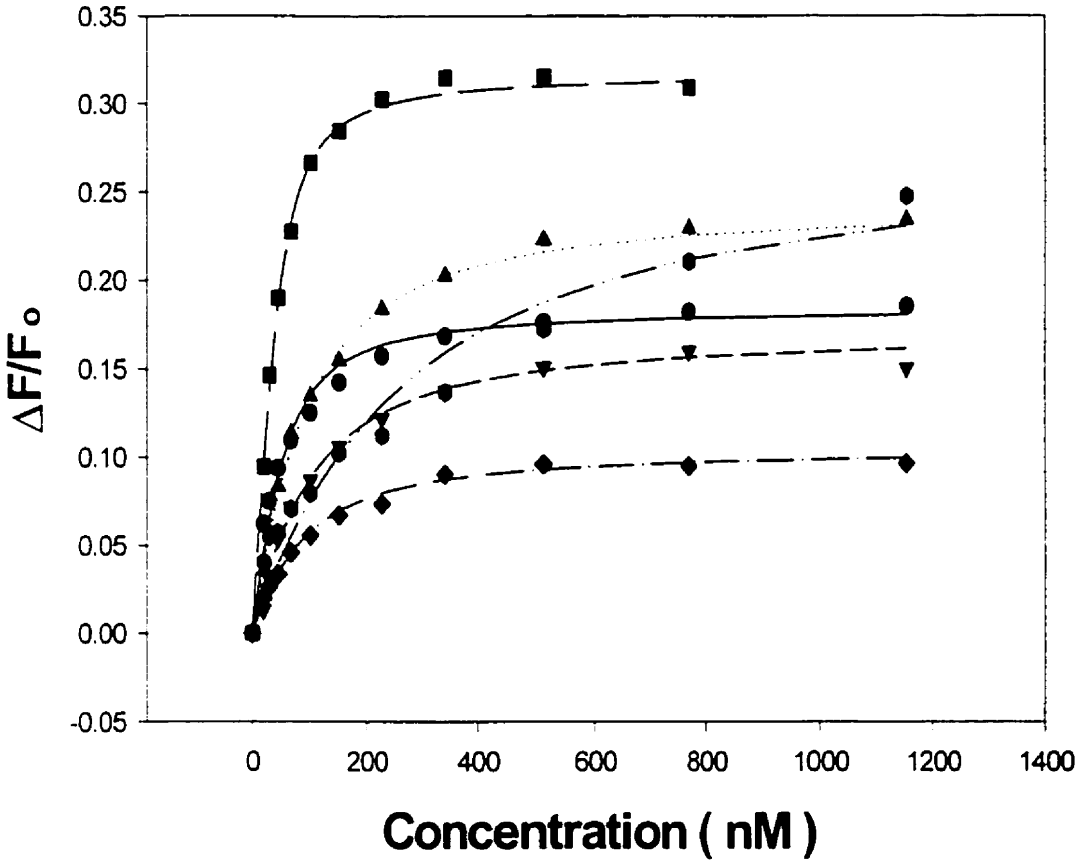

Figure 3.2G

Binding curves of 17K r-apo(a) derivatives to Flu-LDL (50 nM) in solution phase. Symbols represent the absolute value of changes in fluorescence readings over original fluorescence readings, while lines represent the data fit to Equation 1. Circles: 17K wild-type; squares: 17KΔWLBS6; upright triangles: 17KΔWLBS7; inverted triangles: 17KΔWLBS8; diamonds: 17KΔWLBS6,7; hexagons: 17KΔWLBS7,8.

17K r-apo(a) Derivative	K_d value[1] (nM)	Control K_d value[2] (nM)	Relative K_d[3]
17K	23.2 +/- 4.5	---------	---------
17KΔWLBS6	11.4 +/- 1.0	18.6 +/- 5.8	~1X
17KΔWLBS7	61.9 +/- 3.9	27.8 +/- 7.0	~2X
17KΔWLBS8	72.0 +/- 8.3	18.6 +/- 5.8	~4X
17KΔWLBS6,7	60.4 +/- 6.0	18.6 +/- 5.8	~3X
17KΔWLBS7,8	237.2 +/- 72.4	18.6 +/- 5.8	~12.5X

Table 3.1

Comparison of K_d values for 17K r-apo(a) wild-type and mutant derivatives. Data are representative of experiments performed a minimum of two times.

[1]obtained by fitting of fluorescence data to Equation 1.

[2]obtained for 17K wild-type binding experiment performed in parallel.

[3]obtained by comparing K_d value to that of 17K.

3.1.4 Summary of Fluorescent Binding Assay Results

These assays firstly investigated the effect of WLBS mutation in each of KIV_6, KIV_7, and KIV_8 on non-covalent interaction of the corresponding apo(a) derivative and Flu-LDL. The K_d value for the 17KΔWLBS6 derivative binding to Flu-LDL was 11.4 nM, which is compared to the respective 17K wild-type control which yielded a K_d value of 18.6 nM. The data indicate no change in relative K_d value (~1X) compared to the 17K wild-type protein. These results for the mutation of the WLBS in KIV_6, in the context of the 17K apo(a) isoform, indicate that the removal of this WLBS has little effect on the affinity of the initial non-covalent association of apo(a) and apoB. The K_d value for the 17KΔWLBS7 derivative binding to Flu-LDL was 61.9 nM, which is compared to the respective 17K wild-type control which yielded a K_d value of 27.8 nM. The data show an increase in relative K_d value (~2X) compared to the 17K wild-type protein. These results for the mutation of the WLBS in KIV_7, in the context of the 17K apo(a) isoform, indicate that the removal of this WLBS causes an ~2X decrease in affinity of the initial non-covalent association of apo(a) and apoB. The K_d value for the 17KΔWLBS8 derivative binding to Flu-LDL was 72.0 nM, compared to the respective 17K wild-type control which yielded a K_d value of 18.6 nM. The data for this mutant derivative show an increase in relative K_d value (~4X) compared to the 17K wild-type protein. These results for the mutation of the WLBS in KIV_8, in the context of the 17K apo(a) isoform, indicate that the removal of this WLBS causes an ~4X decrease in affinity of the initial non-covalent association of apo(a) and apoB.

We next investigated the effect of WLBS mutation in both KIV_6 and KIV_7, and in both KIV_7 and KIV_8 on the non-covalent interaction of the corresponding apo(a) derivative and Flu-LDL. The K_d value for the 17KΔWLBS6,7 derivative binding to Flu-LDL was 60.4 nM, compared to the respective 17K wild-type control which yielded a K_d value of 18.6 nM. The data show an increase in relative K_d value (~3X) compared to the 17K wild-type protein. These results for the mutation of the WLBS in both KIV_6 and KIV_7, in the context of the 17K apo(a) isoform, indicate that the removal of this WLBS causes an ~3X decrease in affinity of the initial non-covalent association of apo(a) and apoB. The K_d value for the 17KΔWLBS7,8 derivative binding to Flu-LDL was 237.2 nM, compared to the respective 17K wild-type control which yielded a K_d value of 18.6 nM. The data for this mutant derivative show an increase in relative K_d value (~12X) compared to the 17K wild-type protein. These results for the mutation of the WLBS in both KIV_7 and KIV_8, in the context of the 17K apo(a) isoform, indicate that the removal of this WLBS causes an ~12X decrease in affinity of the initial non-covalent association of apo(a) and apoB.

Taken together, the results indicate that removal of the WLBS in KIV_6 does not adversely affect its ability, compared to the 17K wild-type protein, to non-covalently associate with Flu-LDL. Removal of the WLBS in KIV_7 results in decreased binding to Flu-LDL compared to the 17K wild-type protein. Removal of the WLBS in both KIV_6 and KIV_7 results in decreased binding to Flu-LDL compared to 17K wild-type standard, but also when compared to apo(a) with the WLBS removed in KIV_6 and KIV_7 separately. Removal of the WLBS in KIV_8 results in decreased binding to Flu-LDL compared to the

17K wild-type protein, as well as compared to apo(a) derivatives with the WLBS removed in KIV_6 and KIV_7 and simultaneously in KIV_6 and KIV_7. Simultaneous removal of the WLBS in KIV_7 and KIV_8 results in decreased binding to Flu-LDL compared to 17K wild-type standard; this derivative results in the greatest decrease in binding to Flu-LDL compared to the other derivatives. Taken together, these results suggest that the WLBS in KIV_7 and KIV_8, are primarily responsible for the non-covalent interaction with apoB in the first step of Lp(a) assembly. The next stage of this study was to determine if removal of WLBS in 17K apo(a) affects the second step of Lp(a) assembly, the formation of a disulfide bond between apo(a) and apoB. We were also interested in determining whether the results from covalent Lp(a) assembly assays would parallel those observed for the non-covalent assays with respect to which WLBS are important for these processes.

3.2 Covalent Association of Native LDL and 17K r-apo(a) Derivatives

3.2.1 Transient Expression of 17K r-apo(a) Wild-type and Derivatives in Human Embryonic Kidney Cells

The sequences encoding the wild-type 17K r-apo(a) and WLBS mutant derivatives were assembled in the pRK5 expression plasmid (78) as previously described (see Section 2.1). (38) Human embryonic kidney (293) cells transiently expressing 17K r-apo(a) (wild-type and derivatives) were generated by transfection of 293 cells with 10 μg of expression plasmid per 100mm plate by the calcium phosphate co-precipitation

method (see Section 2.2.1). (80) Following transfection, cells were incubated at 37°C in serum-free cultured medium for 48 hours and the corresponding CM was harvested. Levels of expression were determined by ELISA; generally, concentrations ranged from 4 to 8 nM. The CM for each transfection was stored at -20°C prior to covalent binding assays.

3.2.2 Isolation of Native Human LDL

Fresh-frozen plasma, containing 1mM EDTA and 1mM PMSF, was used to isolate LDL by method of sequential flotation, as described previously (see Section 2.3). (83) Protein content was determined utilizing a modified Bradford assay (see Section 2.3) with BSA as a reference standard. Concentrations of native LDL ranged from ~1.0 mg/ml (2.0 μM) to ~2.0 mg/ml (3.9 μM).

3.2.3 Covalent Lp(a) Assembly Assays

CM harvests from transient transfections of the17K r-apo(a) wild type and mutant derivatives were diluted to 2 nM final concentration in HBS containing a 25-fold molar excess of isolated native LDL. Reaction mixtures were incubated at 37°C for 24 hours; at various time points samples were removed for Western blot analysis under non-reduced conditions. Two bands were detected: a lower molecular weight band corresponding to free 17K r-apo(a) wild-type or mutant derivative, and a higher molecular weight species representing the r-apo(a) covalently associated with LDL to form r-Lp(a) particles (see Figure 3.3). Densitometric analysis was used to determine the percentage of apo(a)

incorporated into the Lp(a) particle. Time course curves (see Figures 3.4A, 3.4B, 3.4C, 3.4D, 3.4E, 3.4F) were generated, as previously described. (54) The initial rates of Lp(a) formation were calculated by determining the slopes of the tangents to the initial linear portions of the time course curves, as previously described. (54) The maximum levels of Lp(a) formation were determined by estimation of plateaus for the time course curves over 20 to 24 hours. All experiments were performed a minimum of two times: data shown are from a representative experiment (see Table 3.2).

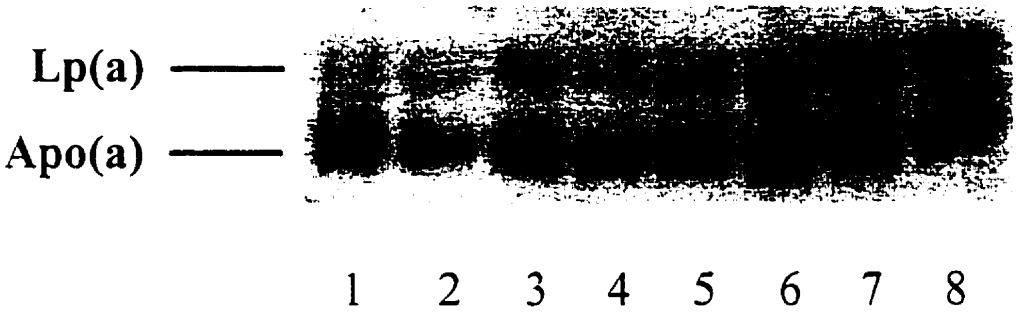

Figure 3.3

Representative analysis for time course of covalent Lp(a) assembly assay. Reaction mixtures consisting of transfected CM and isolated LDL were incubated at 37°C; samples were withdrawn at specified times for analysis by SDS-PAGE on a 6% polyacrylamide gel followed by Western blot analysis. Resulting films were subjected to densitometric analysis in order to determine the intensity of free r-apo(a) and Lp(a) species. Lane 1: 0 hr; Lane 2: 0.5 hr; Lane 3: 1 hr; Lane 4: 2 hr; Lane5: 4 hr; Lane 6: 6 hr; Lane 7: 8 hr; Lane 8: 24 hr.

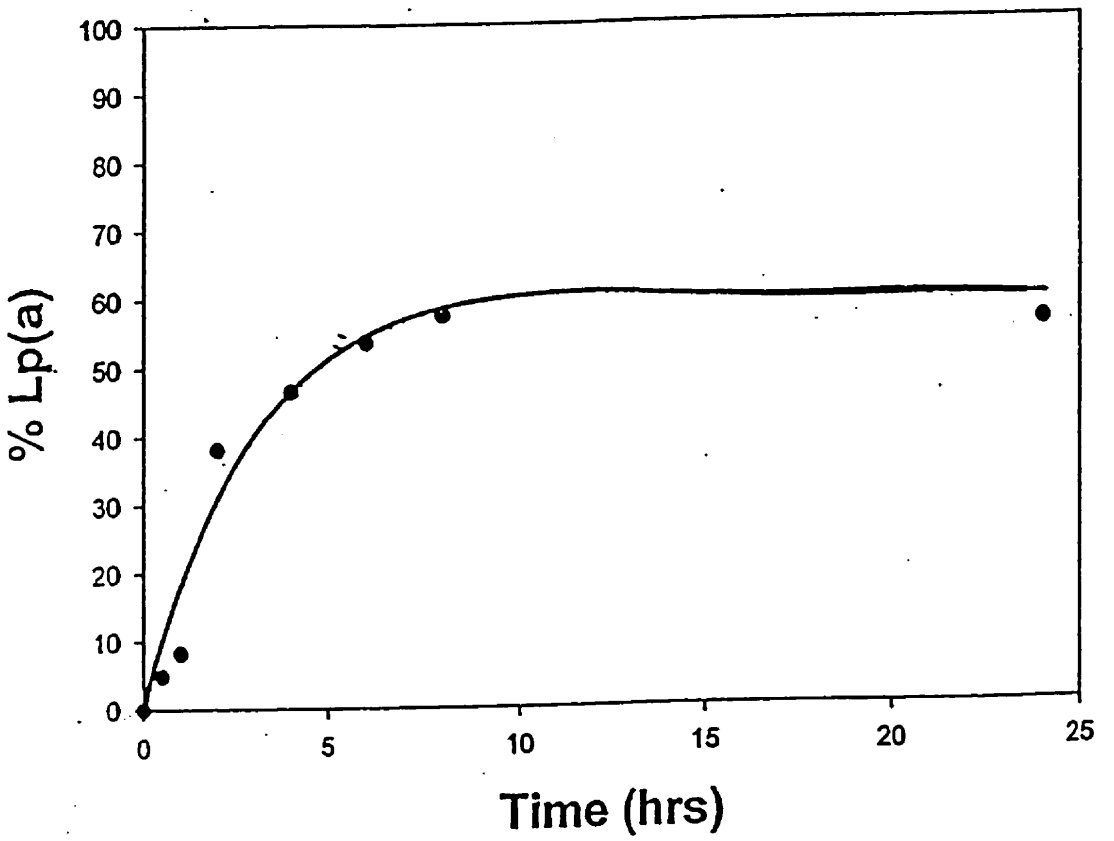

Figure 3.4A

Time course curve for covalent Lp(a) formation using 17K wild-type and LDL. Circles represent percentage of Lp(a) formed at each time point, while the line represents manually fit data. The amount of Lp(a) formed is expressed as a positive percentage of amount of Lp(a) formed with respect to total amount of apo(a) and Lp(a) species at the specified time point. The initial rate of Lp(a) formation (over ~the first two hours) and the estimated maximal Lp(a) formation (after 20 to 24 hours) was determined.

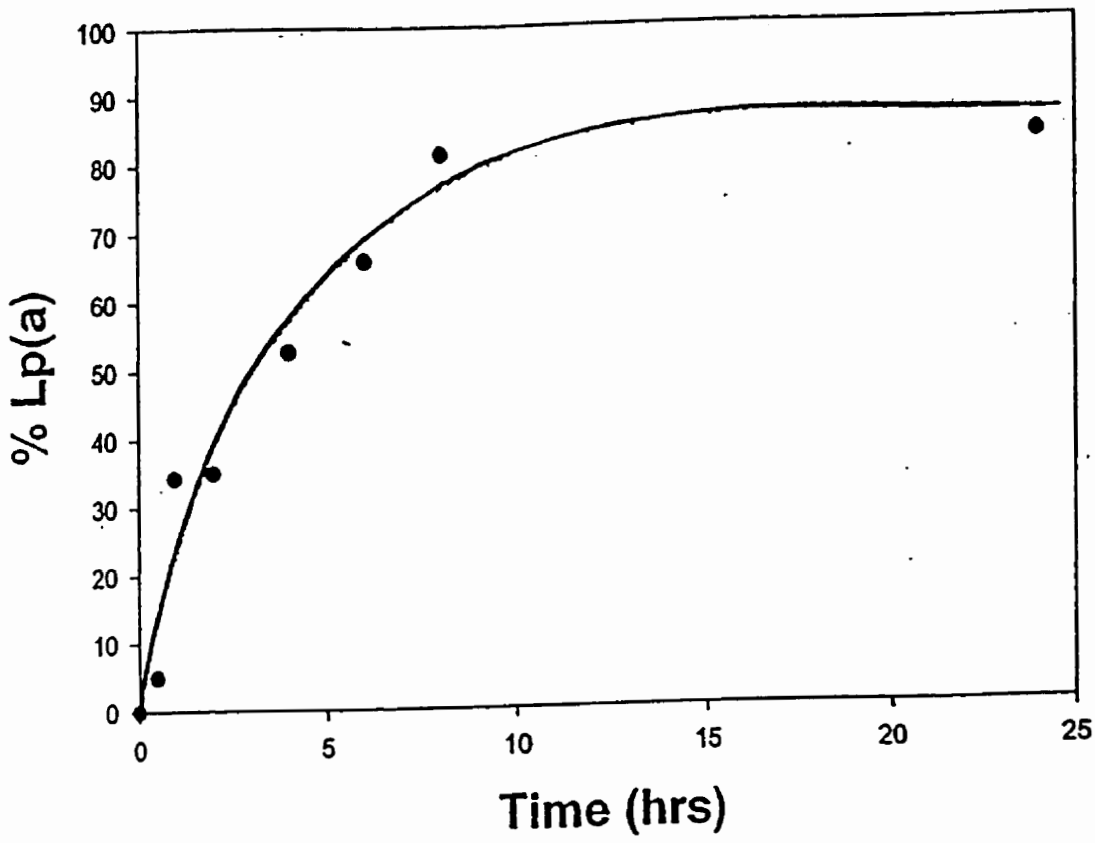

Figure 3.4B

Time course curve for covalent Lp(a) formation using 17KΔWLBS6 and LDL. Circles represent percentage of Lp(a) formed at each time point, while the line represents manually fit data. The amount of Lp(a) formed is expressed as a positive percentage of amount of Lp(a) formed with respect to total amount of apo(a) and Lp(a) species at the specified time point. The initial rate of Lp(a) formation (over ~the first two hours) and the estimated maximal Lp(a) formation (after 20 to 24 hours) was determined.

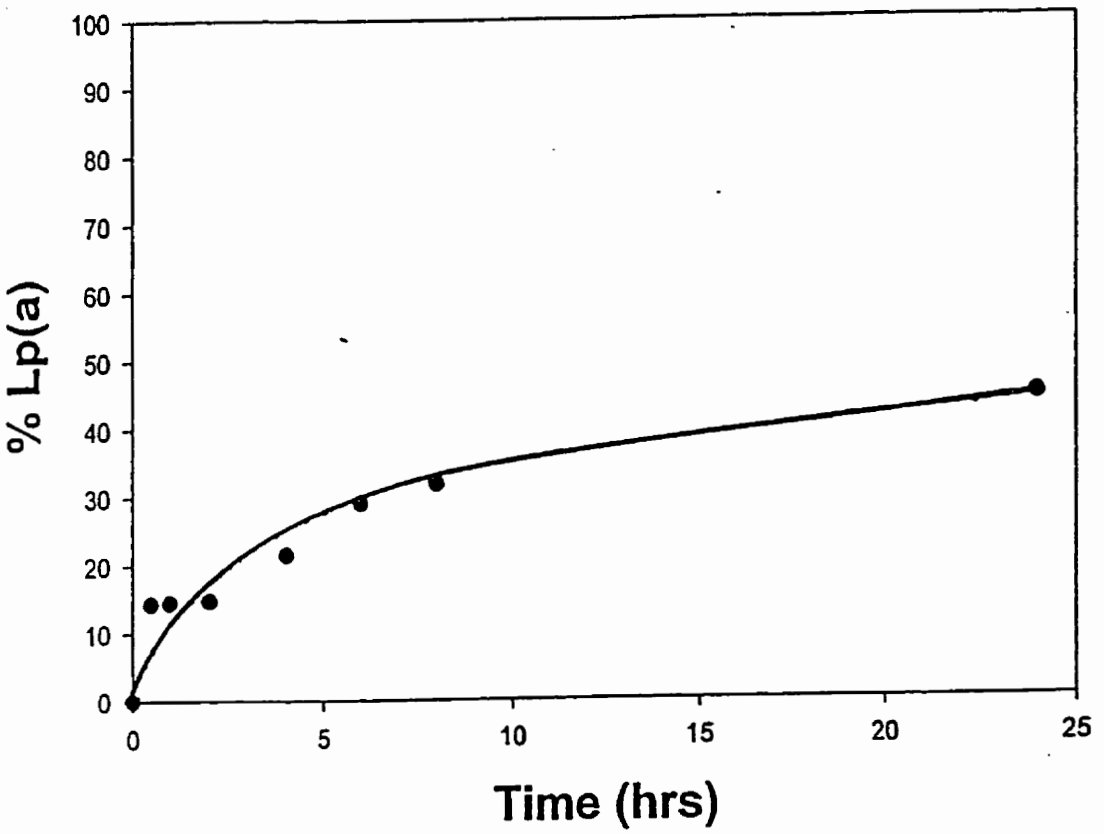

Figure 3.4C

Time course curve for covalent Lp(a) formation using 17KΔWLBS7 and LDL. Circles represent percentage of Lp(a) formed at each time point, while the line represents manually fit data. The amount of Lp(a) formed is expressed as a positive percentage of amount of Lp(a) formed with respect to total amount of apo(a) and Lp(a) species at the specified time point. The initial rate of Lp(a) formation (over ~the first two hours) and the estimated maximal Lp(a) formation (after 20 to 24 hours) was determined.

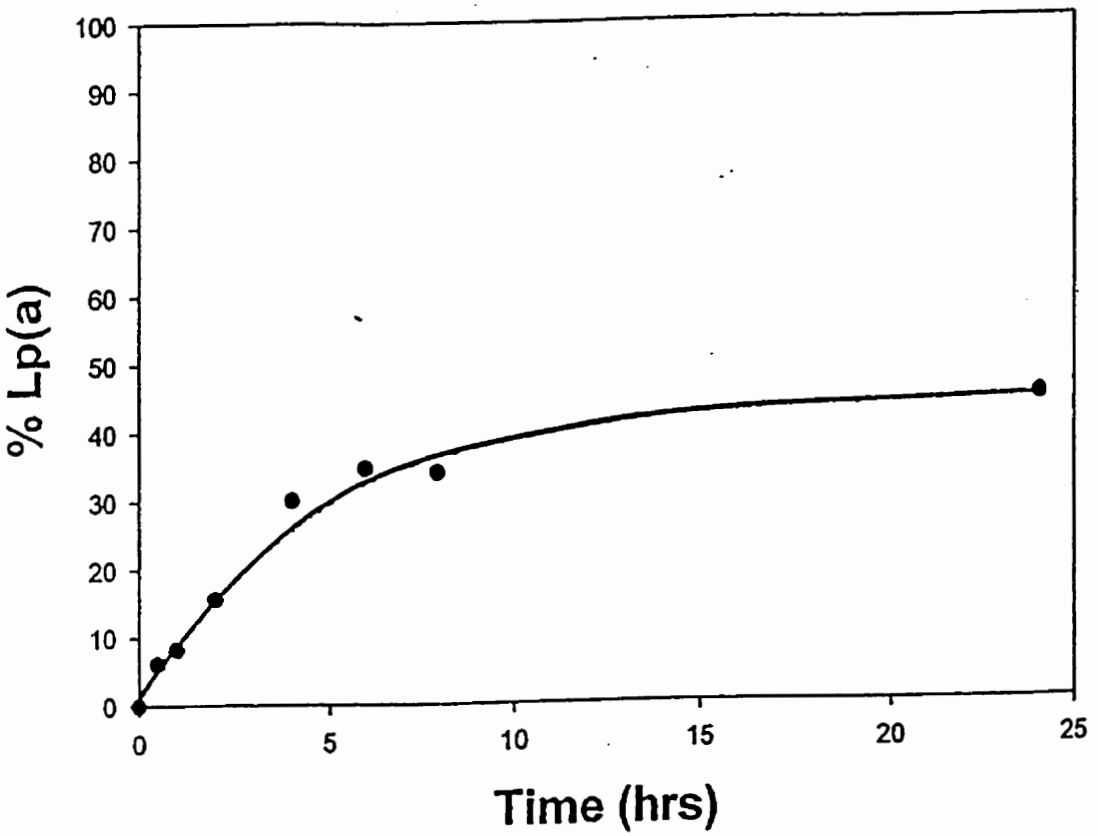

Figure 3.4D

Time course curve for covalent Lp(a) formation using 17KΔWLBS8 and LDL. Circles represent percentage of Lp(a) formed at each time point, while the line represents manually fit data. The amount of Lp(a) formed is expressed as a positive percentage of amount of Lp(a) formed with respect to total amount of apo(a) and Lp(a) species at the specified time point. The initial rate of Lp(a) formation (over ~the first two hours) and the estimated maximal Lp(a) formation (after 20 to 24 hours) was determined.

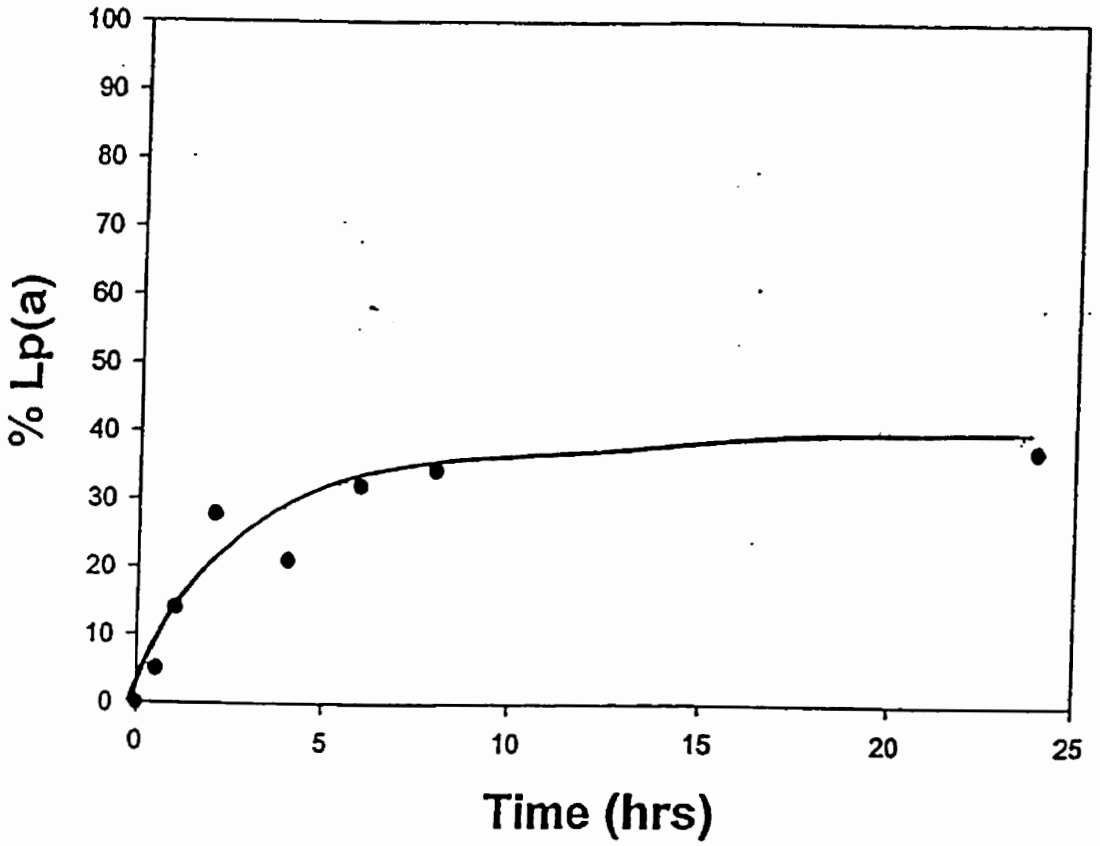

Figure 3.4E

Time course curve for covalent Lp(a) formation using 17KΔWLBS6,7 and LDL. Circles represent percentage of Lp(a) formed at each time point, while the line represents manually fit data. The amount of Lp(a) formed is expressed as a positive percentage of amount of Lp(a) formed with respect to total amount of apo(a) and Lp(a) species at the specified time point. The initial rate of Lp(a) formation (over ~the first two hours) and the estimated maximal Lp(a) formation (after 20 to 24 hours) was determined.

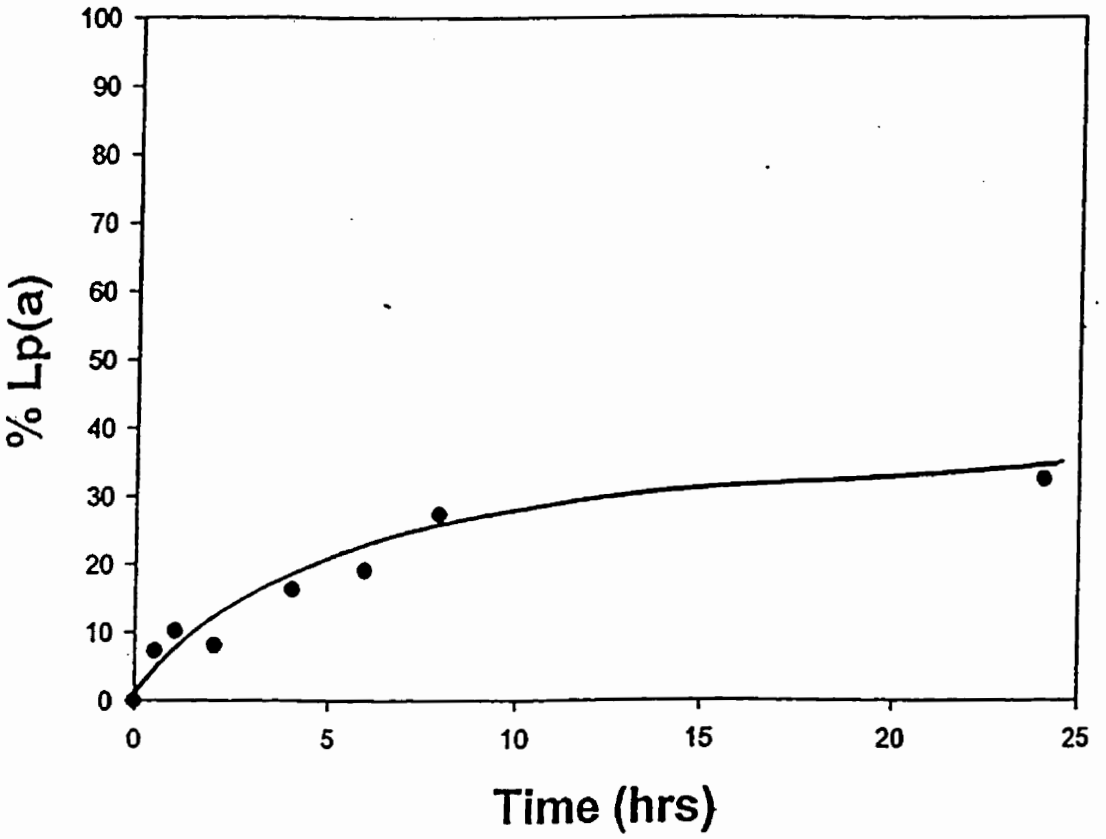

Figure 3.4F

Time course curve for covalent Lp(a) formation using 17KΔWLBS7,8 and LDL. Circles represent percentage of Lp(a) formed at each time point, while the line represents manually fit data. The amount of Lp(a) formed is expressed as a positive percentage of amount of Lp(a) formed with respect to total amount of apo(a) and Lp(a) species at the specified time point. The initial rate of Lp(a) formation (over ~the first two hours) and the estimated maximal Lp(a) formation (after 20 to 24 hours) was determined.

17K r-apo(a) Derivative	Rate of Formation[1] (% hr^{-1})	Relative Rate of Formation[2]	Maximum Formation[3] (%)	Relative Maximum Formation[4]
17K	13.1	---------	~60	---------
17KΔWLBS6	16.2	~1.2X	~85	~1.4X
17KΔWLBS7	8.4	~0.6X	~40	~0.7X
17KΔWLBS8	6.2	~0.5X	~40	~0.7X
17KΔWLBS6,7	9.6	~0.7X	~40	~0.7X
17KΔWLBS7,8	3.9	~0.3X	~30	~0.5X

Table 3.2

Comparison of rates of formation and maximum formation of 17K r-apo(a) wild-type and mutant derivatives. Data are representative of experiments performed a minimum of two times.

[1]obtained by determining slope of the tangent of the covalent Lp(a) assembly curve for each derivative over the initial 2 hr of the time course.

[2]obtained by comparing rate of formation to that of 17K.

[3]obtained by estimating maximum Lp(a) formation between 20 to 24 hr.

[4]obtained by comparing rate of maximum Lp(a) formation to that observed using 17K

3.2.4 Summary of Covalent Binding Assay Results

These assays firstly investigated the effect of WLBS mutation in each of KIV_6, KIV_7, and KIV_8 on the covalent bond formation between the corresponding apo(a) derivative and native LDL. The initial rate of Lp(a) formation for the 17KΔWLBS6 derivative with LDL was 16.2 $\%h^{-1}$, compared to the respective 17K wild-type control which yielded an initial rate of Lp(a) formation of 13.1 $\%h^{-1}$. The maximum level of Lp(a) formation for the 17KΔWLBS6 derivative with LDL was ~85%, compared to the respective 17K wild-type control which yielded a maximum level of Lp(a) formation of ~60%. An increase was observed in both relative rate of Lp(a) formation (~1.2X) and relative maximum Lp(a) formation (~1.4X) compared to that observed using the 17K wild-type protein. These results for the mutation of the WLBS in KIV_6, in the context of the 17K apo(a) isoform, indicate that the removal of this WLBS promotes both the rate and extent of Lp(a) formation. The initial rate of Lp(a) formation for the 17KΔWLBS7 derivative with LDL was 8.4 $\%h^{-1}$, compared to the respective 17K wild-type control which yielded an initial rate of Lp(a) formation of 13.1 $\%h^{-1}$. The maximum level of Lp(a) formation for the 17KΔWLBS7 derivative with LDL was ~40%, compared to the respective 17K wild-type control which yielded a maximum level of Lp(a) formation of ~60%. An increase was observed in both relative rate of Lp(a) formation (~0.6X) and relative maximum Lp(a) formation (~0.7X) compared to that observed using the 17K wild-type protein. These results for the mutation of the WLBS in KIV_7, in the context of the 17K apo(a) isoform, indicate that the removal of this WLBS results in a decrease in both the rate and extent of Lp(a) formation. The initial rate of Lp(a) formation for the

17KΔWLBS8 derivative with LDL was 6.2 $\%h^{-1}$, compared to the respective 17K wild-type control which yielded an initial rate of Lp(a) formation of 13.1 $\%h^{-1}$. The maximum level of Lp(a) formation for the 17KΔWLBS8 derivative with LDL was ~40%, compared to the respective 17K wild-type control which yielded a maximum level of Lp(a) formation of ~60%. An increase was observed in both relative rate of Lp(a) formation (~0.5X) and relative maximum Lp(a) formation (~0.7X) compared to that observed using the 17K wild-type protein. These results for the mutation of the WLBS in KIV_8, in the context of the 17K apo(a) isoform, indicate that the removal of this WLBS also decreases both the rate and extent of Lp(a) formation.

We next investigated the effect of WLBS mutation in both KIV_6 and KIV_7, and in both KIV_5 and KIV_8 on the covalent bond formation between the corresponding apo(a) derivatives and native LDL. The initial rate of Lp(a) formation for the 17KΔWLBS6,7 derivative with LDL was 9.6 $\%h^{-1}$, compared to the respective 17K wild-type control which yielded an initial rate of Lp(a) formation of 13.1 $\%h^{-1}$. The maximum level of Lp(a) formation for the 17KΔWLBS6,7 derivative with LDL was ~40%, compared to the respective 17K wild-type control which yielded a maximum level of Lp(a) formation of ~60%. An increase was observed in both relative rate of Lp(a) formation (~0.7X) and relative maximum Lp(a) formation (~0.7X) compared to that observed using the 17K wild-type protein. These results for the mutation of the WLBS in both KIV_6 and KIV_7, in the context of the 17K apo(a) isoform, indicate that the removal of these WLBS decreases both the rate and extent of Lp(a) formation. The initial rate of Lp(a) formation for the 17KΔWLBS6,7 derivative with LDL was 3.9 $\%h^{-1}$, compared to the respective 17K wild-

type control which yielded an initial rate of Lp(a) formation of 13.1 $\%\cdot h^{-1}$. The maximum level of Lp(a) formation for the 17KΔWLBS6,7 derivative with LDL was ~30%, compared to the respective 17K wild-type control which yielded a maximum level of Lp(a) formation of ~60%. An increase was observed in both relative rate of Lp(a) formation (~0.3X) and relative maximum Lp(a) formation (~0.5X) compared to that observed using the 17K wild-type protein. These results for the mutation of the WLBS in both KIV_6 and KIV_8, in the context of the 17K apo(a) isoform, indicate that the removal of these WLBS also decreases both the rate and extent of formation of a covalent bond between apo(a) and apoB.

These results indicate that removal of the WLBS in KIV_6 resulted in a slight increase in both rate and extent of Lp(a) formation compared to that observed using the 17K wild-type protein. Removal of the WLBS in KIV_7 resulted in a decrease in both rate and extent of Lp(a) formation compared to that observed using the 17K wild-type protein. Removal of the WLBS in both KIV_6 and KIV_7 resulted in a decrease in both rate and extent of Lp(a) formation compared to that observed using the 17K wild-type protein; this mutant derivative exhibited a slight increase in rate and no change in extent of Lp(a) formation compared to that observed using the 17KΔWLBS7 and exhibited decreases in both rate and extent of Lp(a) formation compared to that observed using the 17KΔWLBS6. Removal of the WLBS in KIV_8 resulted in a decrease in both rate and extent of Lp(a) formation compared to that observed using the 17K wild-type protein; this mutant derivative exhibited a decrease in rate of Lp(a) formation compared to that observed using the 17KΔWLBS6, 17KΔWLBS7 and 17KΔWLBS6,7. The 17KΔWLBS8

also exhibited a decrease in extent of Lp(a) formation compared to 17KΔWLBS6, but exhibited no change compared to 17KΔWLBS7 and 17KΔWLBS6,7. Removal of the WLBS in both KIV$_7$ and KIV$_8$ resulted in a decrease in both rate and extent of Lp(a) formation compared to that observed using the 17K wild-type protein; this derivative resulted in the greatest decrease in these parameters compared to the other derivatives. Taken together, these results suggest that the WLBS in KIV$_7$ and KIV$_8$ are primarily responsible for mediating the non-covalent apo(a)-apoB interaction and ultimately covalent Lp(a) formation. The results of the non-covalent and covalent assays in the current study are in good agreement. This suggests that the first step of Lp(a) assembly (i.e. the non-covalent association of apo(a) and apoB) dictates the efficiency to which the second step (i.e. formation of the covalent bond between apo(a) and apoB-100) occurs.

Discussion

4.1 Model for Lp(a) Assembly

Lp(a) consists of apoB disulfide bonded to apo(a) (see Section 1.2), in a 1:1 molar ratio. (18) The Cys3734 residue of apoB100 may be involved in the disulfide linkage with apo(a) (see Section 1.5.4), although this remains controversial. (16,67) The apo(a) cysteine involved in disulfide linkage to apoB has been conclusively identified as Cys4057, the seventh unpaired cysteine in KIV_9 (see Section 1.5.5) (45,46) Lp(a) assembly has been determined to be a two step process (53), in which initial non-covalent association of apo(a) and apoB is followed by the formation of a covalent bond between the two species (see Figure 1.5); the non-covalent step is sensitive to the addition of lysine and lysine analogues. (54,64,66) A number of studies have been performed to date in order to establish which sequences in apo(a) and apoB are required for Lp(a) assembly. The presence of WLBS in each of apo(a) KIV_5 to KIV_8 have been demonstrated (52); several studies suggest that sequences within apo(a) KIV_6, KIV_7 and KIV_8 are required for non-covalent interaction with apoB (52,63,64,76), while other studies (54,66) suggest that sequences within apo(a) KIV_7 and KIV_8 are required for this interaction and that KIV_6 plays only a minor role in Lp(a) assembly. Other studies (53,77) suggest that apo(a) KIV_6 and KIV_7 are the major kringles involved in the initial non-covalent interaction with apoB100 to form Lp(a) particles. Frank *et al* demonstrated that the spacing or distance between KIV_5 and KIV_9 is important, with a required length corresponding to two KIV sequences. (75) This gives credence to the current study in that conformational integrity of a physiologically-relevant r-apo(a) may be important in Lp(a) assembly. All of these

studies utilized truncated forms of apo(a); the objective of the current study was to determine the effect of the affinity reduction of WLBS in apo(a) KIV_6, KIV_7 and KIV_8 in the context of 17K apo(a) which corresponds to a physiologically-occurring isoform. In order to directly demonstrate the role of WLBS in the context of 17K r-apo(a) we generated mutations in these WLBS (see Section 2.1) and assessed their ability to bind non-covalently to LDL and to form covalent Lp(a) particles.

4.1.1 Role of WLBS of 17K r-Apo(a) on Non-covalent Lp(a) Assembly

Studies from our laboratory have shown that sequences within KIV_6, KIV_7 and KIV_8 appear to be required for the initial non-covalent interaction with apoB and that these sequences bind directly to immobilized LDL in a lysine-dependent manner. (66,76) Based on studies using truncated apo(a) derivatives (see Section 1.5.5 and Section 4.1), it is controversial whether KIV_6, KIV_7 and KIV_8 only play a direct lysine-binding role in the initial non-covalent step of Lp(a) assembly, or whether they also exert their effects indirectly through a conformational stabilization of other C-terminal sequences. Also, it is unclear whether other sequences in addition to WLBS in these kringles are required for Lp(a) assembly. To address these questions, the current study utilized WLBS mutants generated in the context of 17K r-apo(a) rather than truncated derivatives. Isolated human LDL was fluorescently-labeled with 5'-IAF which tags free, exposed cysteines. This effectively abolishes the ability of LDL and apo(a) to form a covalent Lp(a) particle in our assay. Also, the temperature and time requirements for covalent Lp(a) particle formation (see Section 2.4.3) are not favourable for covalent Lp(a) formation. Binding

affinities of the various derivatives for Flu-LDL were obtained (see Section 3.1.3) and compared to the 17K wild-type r-apo(a) performed in parallel (see Table 3.1).

The current study firstly investigated the effect of WLBS mutation in each of KIV_6, KIV_7 and KIV_8 on non-covalent interaction of the corresponding apo(a) derivative and Flu-LDL. We found that the K_d value for the 17KΔWLBS6 binding to Flu-LDL is comparable to the respective 17K wild-type control. These results for the mutation of the WLBS in KIV_6, in the context of the 17K apo(a) isoform, indicate that removal of this WLBS has very little effect on the affinity of the initial non-covalent association of apo(a) and apoB. Our data indicate that the K_d value for the 17KΔWLBS7 binding to Flu-LDL is ~2X greater compared to the respective 17K wild-type control. These results for the mutation of the WLBS in KIV_7, in the context of the 17K apo(a) isoform, indicate that the removal of this WLBS causes an ~2X decrease in affinity of the initial non-covalent association of apo(a) and apoB. The K_d value for the 17KΔWLBS8 binding to Flu-LDL is ~4X greater compared to the respective 17K wild-type control. These results for the mutation of the WLBS in KIV_8, in the context of the 17K apo(a) isoform, indicate that the removal of this WLBS causes an ~4X decrease in affinity of the initial non-covalent association of apo(a) and apoB. These results, using single point mutations in the 17K apo(a) isoform, indicate that the non-covalent binding affinity of apo(a) for apoB is largely mediated by KIV_7 and KIV_8, with KIV_8 WLBS having the greatest role. The current study contradicts a previous study using truncated r-apo(a) derivatives (76) which also suggested a role for KIV_6 in the non-covalent association of apo(a) and apoB-100. An additional study which utilized truncated r-apo(a) species (53) suggested that KIV_6

primarily mediates the interaction of apo(a) and apoB. Previous work from our laboratory (66) also demonstrated a small role for KIV_9 in the non-covalent interaction of apo(a) and apoB, which has been substantiated by addition studies from our lab. (74)

We next investigated the effect of mutation of the WLBS in both KIV_6 and KIV_7, and in both KIV_7 and KIV_8 on non-covalent interaction of apo(a) and apoB. The K_d value for the 17KΔWLBS6,7 binding to Flu-LDL is ~3X greater compared to the respective 17K wild-type control. These results for the mutation of the WLBS in both KIV_6 and KIV_7, in the context of the 17K apo(a) isoform, indicate that the removal of these WLBS causes an ~3X decrease in affinity of the initial non-covalent association of apo(a) and apoB. The K_d value for the 17KΔWLBS7,8 binding to Flu-LDL is ~12.5X greater compared to the respective 17K wild-type control. These results for the mutation of the WLBS in both KIV_7 and KIV_8, in the context of the 17K apo(a) isoform, indicate that the removal of these WLBS causes an ~12.5X decrease in affinity of the initial non-covalent association of apo(a) and apoB. These results, using point mutations in combination in the 17K apo(a) isoform, also indicate that the WLBS in KIV_7 and KIV_8 are both required for maximally efficient non-covalent Lp(a) assembly. We observed that the affinity reduction of the WLBS in both KIV_6 and KIV_7 results in a greater decrease in affinity of the apo(a)-apoB interaction when compared to that observed upon mutation of the WLBS in either KIV_6 or KIV_7. The mutation of the WLBS in both KIV_6 and KIV_7 results in a lesser decrease in affinity of apo(a) and apoB when compared to the mutation of the WLBS in KIV_8, again pointing to a key role for the WLBS in KIV_8 in mediating non-covalent interactions with apoB. While our data suggests no role for KIV_6 in non-

covalent Lp(a) assembly, simultaneous removal of the WLBS in both KIV_6 and KIV_7 has a slightly greater effect than removal of the WLBS in KIV_7 alone. This suggests that KIV_6 plays a synergistic role with KIV_7. The mutation of the WLBS in both KIV_7 and KIV_8, in the context of the 17K apo(a) isoform, resulted in the greatest decrease in affinity of apo(a) to apoB compared to all other derivatives used in the current study. Our data suggest a role for KIV_7 and for KIV_8 in non-covalent Lp(a) assembly, while simultaneous removal of the WLBS in both KIV_7 and KIV_8 suggests that these effects can act synergistically to drastically decrease the affinity of the apo(a)-apoB interaction. This contradicts previous studies (53,76) that specifically implicate KIV_6 and KIV_7 in initial non-covalent apo(a)-apoB interaction.

The results of the current study suggest that the WLBS in KIV_7 and KIV_8 play the greatest role in mediating non-covalent apo(a) and apoB interactions. We now wanted to test the validity of the two-step model of Lp(a) assembly, which predicts that these mutations will also affect covalent Lp(a) assembly.

4.1.2 Role of WLBS of 17K r-Apo(a) on Covalent Lp(a) Assembly

As mentioned above (see Section 4.1.1) several studies (53,66,76) have suggested the importance of either KIV_6, KIV_7, KIV_8, or a combination of these on the initial non-covalent step of Lp(a) assembly. Several other studies (54,75,77,84) have focused on the second step of Lp(a) assembly, that of covalent bond formation between apo(a) and apoB, primarily using truncated apo(a) derivatives. In the current study we utilized WLBS mutant derivatives in the context of the 17K r-apo(a) rather than truncated species. Initial

rates of reaction and maximal levels of Lp(a) formation of the various derivatives were obtained (see Section 3.2.3) and compared to that obtained using the 17K wild-type r-apo(a) performed in parallel (see Table 3.2).

We investigated the effect of WLBS mutation in each of KIV_6, KIV_7 and KIV_8 on covalent formation of Lp(a) particle by SDS-PAGE under non-reducing conditions followed by Western blotting (see Section 2.4.3) The initial rate of Lp(a) formation for the 17KΔWLBS6 derivative and LDL is ~1.2X greater compared to the respective 17K wild-type control. Also, the maximum percentage of formation for the 17KΔWLBS6 derivative and LDL is ~1.4X greater compared to the respective 17K wild-type control. These results for the mutation of the WLBS in KIV_6, in the context of the 17K apo(a) isoform, indicate that the removal of this WLBS slightly increases the ability, both in rate and extent, of apo(a) and apoB to covalently associate. The initial rate of Lp(a) formation for the 17KΔWLBS7 derivative and LDL is ~0.6X less compared to the respective 17K wild-type control. Also, the maximum percentage of formation for the 17KΔWLBS7 derivative and LDL is ~0.7X less compared to the respective 17K wild-type control. These results for the mutation of the WLBS in KIV_7, in the context of the 17K apo(a) isoform, indicate that the removal of this WLBS decreases the ability, both in rate and extent, of apo(a) and apoB to covalently associate. The initial rate of Lp(a) formation for the 17KΔWLBS8 derivative and LDL is ~0.5X less compared to the respective 17K wild-type control. Also, the maximum percentage of formation for the 17KΔWLBS8 derivative and LDL is ~0.7X less compared to the respective 17K wild-type control. These results for the mutation of the WLBS in KIV_8, in the context of the 17K apo(a)

isoform, indicate that the removal of this WLBS decreases the ability, both in rate and extent, of apo(a) and apoB to covalently associate. These results, using single point mutations in the 17K apo(a) isoform, indicate that the initial rate and extent of covalent assembly of apo(a) and apoB is primarily mediated by the WLBS in KIV_8 with lesser contributions from the WLBS in KIV_7 and KIV_6, respectively. This is in complete agreement with non-covalent binding data generated in the current study, which validates the two-step model for Lp(a) assembly. The current study contradicts several other studies using truncated r-apo(a) derivatives which suggest a major role for KIV_6 (75) or both KIV_6 and KIV_7 (77,84) in covalent formation of Lp(a). The current study is in agreement, however with previous studies from this laboratory. (54) In the latter study, sequential removal of N-terminal kringle domains was performed and effects on covalent Lp(a) formation were analyzed using the same methodology as in the current study. Removal of KIV_6 did not affect rate and extent of Lp(a) particle formation, while removal of KIV_7 caused a decrease in both rate and extent of Lp(a) particle formation. An even further decrease in rate and extent were observed upon removal of KIV_8. The results of this study support those of the current study in which the WLBS in KIV_8 plays a major role in covalent Lp(a) formation, with lesser contributions from the WLBS in KIV_7 and KIV_6, respectively.

We next investigated the effect of WLBS mutation in both KIV_6 and KIV_7, and in both KIV_7 and KIV_8 on covalent formation of Lp(a). The initial rate of Lp(a) formation for the 17KΔWLBS6,7 derivative and LDL is ~0.7X less compared to the respective 17K wild-type control. Also, the maximum percentage of formation for the 17KΔWLBS6,7

derivative and LDL is ~0.7X less compared to the respective 17K wild-type control. These results for the simultaneous mutation of the WLBS in KIV_6 and KIV_7 in the context of the 17K apo(a) isoform, indicate that the removal of these WLBS decreases the ability, both in rate and extent, of apo(a) and apoB to covalently associate. The initial rate of Lp(a) formation for the 17KΔWLBS7,8 derivative and LDL is ~0.3X less compared to the respective 17K wild-type control. Also, the maximum percentage of formation for the 17KΔWLBS6,7 derivative and LDL is ~0.5X less compared to the respective 17K wild-type control. These results for the simultaneous mutation of the WLBS in KIV- and KIV_8 in the context of the 17K apo(a) isoform, indicate that the removal of these WLBS decreases both rate and extent of Lp(a) formation. These results are also in agreement with non-covalent binding data obtained using these apo(a) derivatives. We observed that the mutation of the WLBS in both KIV_6 and KIV_7 resulted in a greater decrease in initial rate of covalent Lp(a) assembly compared to the mutation of the WLBS in KIV_6 alone, but a lesser decrease in initial rate of covalent Lp(a) assembly when compared to the mutation of the WLBS in KIV_7 alone. However, the simultaneous mutation of the WLBS in both KIV_6 or KIV_7 resulted in a lesser decrease in initial rate of covalent Lp(a) assembly compared to the mutation of the WLBS in KIV_8. We also observed that the mutation of the WLBS in both KIV_6 and KIV_7 results in a greater decrease extent of covalent Lp(a) assembly compared to the mutation of the WLBS in KIV_6, while no change in extent of covalent Lp(a) assembly was observed compared to the data generated for the mutation of the WLBS in KIV_7. The simultaneous mutation of the WLBS in both KIV_6 and KIV_7 results in a greater decrease in extent of

covalent Lp(a) assembly compared to the mutation of the WLBS in KIV_8. Our results suggest that the WLBS in KIV_6 is not required for covalent Lp(a) assembly. Point mutations in the WLBS in both KIV_6 and KIV_7 also suggest that KIV_6 does not mediate covalent Lp(a) assembly. The simultaneous mutation of the WLBS in both KIV_7 and KIV_8 results in the greatest decrease in rate and extent of covalent Lp(a) formation compared to all other derivatives used in the current study. Mutations in the WLBS in either KIV_7 or KIV_8 suggest a role for the WLBS in these kringles in covalent Lp(a) assembly; results for the simultaneous removal of WLBS in KIV_7 and KIV_8 suggest that these WLBS can act synergistically in mediating Lp(a) assembly. The results for the double WLBS mutations also contradict several other studies that suggest KIV_6 (75) or both KIV_6 and KIV_7 (77,84) primarily mediate covalent Lp(a) formation.

The data for the non-covalent and covalent Lp(a) formation that we have generated suggest a role for the WLBS in both KIV_7 and KIV_8 in these processes. The first step of Lp(a) assembly is mediated primarily by WLBS in KIV_7 and KIV_8, while the second step, covalent Lp(a) assembly, is dictated by non-covalent interactions between KIV_7 and KIV_8 of apo(a) and LDL.

4.1.3 Reliability of Assays

Previous studies (52,53,54,63,64,66,76,77) have utilized apo(a) derivatives with particular KIV domains removed by truncation in order to study the role of these domains in apo(a)-apoB interaction. The effect of truncations on the formation of apo(a) is unknown and may affect its interaction with apoB. The current study uses

physiologically-relevant apo(a) isoforms containing site-specific mutations, thereby minimizing structural alterations of the apo(a). Additionally, both non-covalent and covalent assays were performed in solution phase promoting the native conformation and interaction of apo(a) and apoB. However, the non-covalent assays require a fluorescent label on the free cysteine of LDL, which prevents covalent association of apo(a) and apoB, but which may also affect non-covalent interactions. The utilization of a smaller-sized fluorescent label at the same position on LDL and subsequent labeling of LDL at a differing position could help determine whether the current labeling method is valid. The affinity of 17K for LDL in the current study is comparable to that obtained for an immobilized system using iodinated apo(a). (B. Gabel, unpublished data) Covalent assays utilize native LDL and allow for the formation of a disulfide bond with apo(a). The current and a previous study (54) were unable to demonstrate complete incorporation of 17K r-apo(a) into Lp(a) particle. Addition of hepatocyte membrane increases the amount of 17K r-apo(a) able to be incorporated into the Lp(a) particle (T.G. Wright, unpublished data), suggesting conditions could be optimized for covalent assembly assays. In the densitometric analysis of covalent Lp(a) formation the same antibody is used to detect free apo(a) and apo(a) in the Lp(a) particle. This assumes that apo(a) is detected with the same efficiency in its bound state as in its free state; this assumption should be tested. Also, use of the phosphoimager rather than X-ray film for detection may improve the sensitivity and accuracy of the subsequent densitometric analysis. The current results for non-covalent Lp(a) assembly parallel results for covalent Lp(a) assembly, suggesting that the assays are valid.

4.2 Revised Model for Lp(a) Assembly

As previously mentioned (see Section 4.1), Lp(a) assembly has been determined to be a two step process, in which initial non-covalent association of apo(a) and apoB is followed by the formation of a covalent bond between the two species (see Figure 1.5). (53) A number of studies (52,53,54,63,66,76,77) have been performed to establish which sequences in apo(a) and apoB are required for Lp(a) assembly; these studies have been used to establish a more refined model for this process. One such study (75) suggests that KIV_5 mediates the interaction of apo(a) and apoB. Another study (53) also demonstrated a role for KIV_6 with KIV_7 contributing to a lesser degree. Other studies (77,84) also showed KIV_6 and KIV_7 as being crucial for apo(a)-apoB interactions in Lp(a) assembly. Previous work in our lab (54,76) has contributed to the refinement of the two-step model by the use of apo(a) truncations for binding studies. Results from the non-covalent study by Gabel *et al* (76) suggest a role for sequences within KIV_6, KIV_7 and KIV_8 in Lp(a) assembly, while results from an additional study by Gabel and co-workers (54) suggest a role for KIV_7 and KIV_8 in covalent Lp(a) assembly. The current study specifically examined the role of WLBS in apo(a) KIV_6, KIV_7 and KIV_8 in both non-covalent and covalent Lp(a) assembly, in the context of the physiologically-relevant 17K apo(a) isoform. As such, results from the current study are in partial agreement with the non-covalent results from Gabel *et al* (76), but are in complete agreement with the covalent Lp(a) formation studies (54) which demonstrated that apo(a) KIV_7 and KIV_8 domains both play a crucial role in covalent Lp(a) assembly. Also, the agreement between non-covalent and covalent data in the current study demonstrates that the second step of Lp(a)

assembly is effectively dictated by the efficiency of the initial non-covalent interaction between apo(a) and LDL. Since previous studies utilized truncated forms of apo(a) while the current study utilizes a physiologically-relevant apo(a) isoform containing single amino acid substitutions, we consider the present study to be more reliable. As such, we are now proposing a modified model of the Lp(a) assembly mechanism. (see Figure 4.1).

4.3 Future Directions

From the present study, it has been determined that KIV_7 and KIV_8 play the greatest role in mediating the apo(a)-apoB interaction. As such, these sequences should be further studied. We have expressed apo(a) KIV_7 in *E. coli* and solved the crystal structure; we now plan to express KIV_8 and determine the structure of its WLBS. This will help to develop an understanding of how these WLBS participate in Lp(a) formation. For example, it will be of interest to determine whether or not there are fundamental differences in the WLBS of KIV_7 and KIV_8, or whether the greater contribution of KIV_8 to the process of Lp(a) assembly reflects its position relative to KIV_9. Several amino acids and compounds are known to inhibit the non-covalent interaction of apo(a) and apoB. Non-covalent fluorescence assays may be repeated using the apo(a) derivatives with subsequent addition of these inhibitors in order to analyze their effects on binding affinities. Also, these inhibitors could be analyzed for their effect on covalent Lp(a) assembly using the apo(a) derivatives described in this study.

The sequences in apoB which are required for its interaction with apo(a) are also being studied in our lab. This information will help to provide a more complete

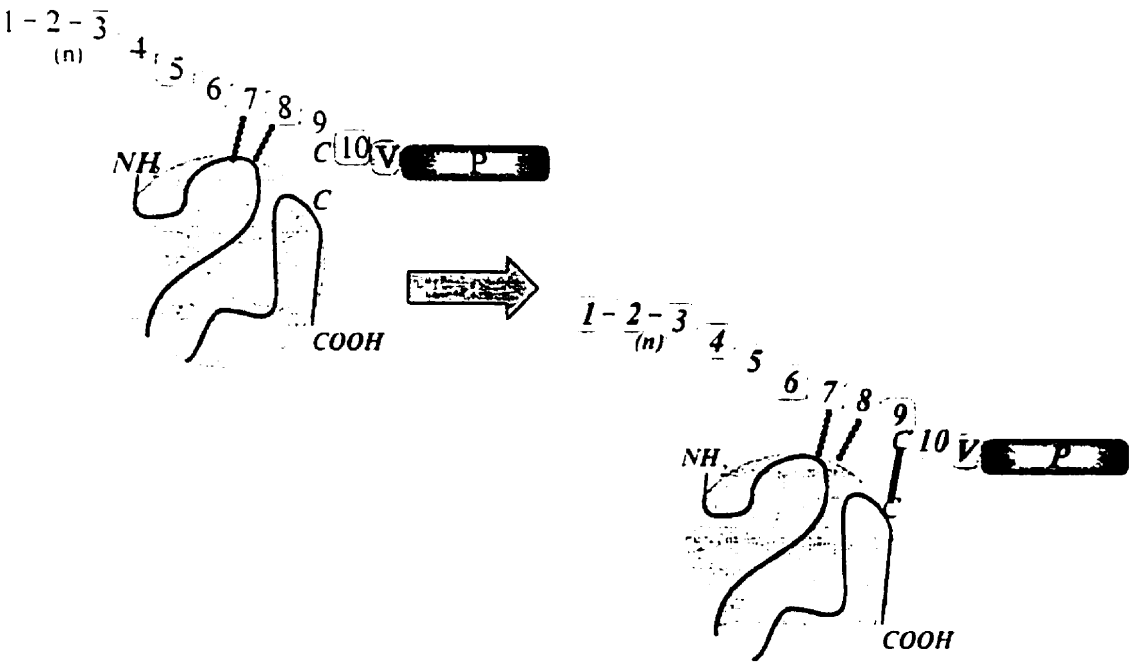

Figure 4.1

Revised schematic representation of the two step Lp(a) assembly model. Weak lysine binding sites in KIV_{7-8} associate non-covalently with apoB. In this model, the initial non-covalent association aligns KIV_9 of apo(a) with a free cysteine in apoB (Cys3734). A covalent disulfide bond is formed between the two proteins, completing the second step of Lp(a) assembly.

understanding of the process of Lp(a) assembly. The long-term benefit of this knowledge could be to develop precise inhibitors used to prevent the formation of Lp(a), thereby reducing the levels of this atherogenic lipoprotein in plasma.

References

1. Berg, K. (1963) *Acta. Pathol. Microbiol. Scand.* 59:369-382.

2. Marcovina, S.M., and Koschinsky, M.L. (1998) *Am. J. Cardiol.* 82:57U-66U.

3. Fan, J., Araki, M., Wu, L., Challah, M., Shimoyamada, H., Lawn, R.M., Kakuta, H., Shikama, H., and Watanabe, T. (1999) *Biochem. Biophys. Res. Comm.* 255:639-644.

4. Koschinksy, M.L., and Marcovina, S.M. (1997) *Int. J. Clin. Lab. Res.* 27:14-23.

5. Dahlén, G.H., and Stenlund, H. (1997) *Clin. Genet.* 52:272-280.

6. Utermann, G., Menzel, H.J., Kraft, H.G., Duba, H.C., Kemmler, H.G., and Seitz, C. (1987) *J. Clin. Invest.* 80:458-465.

7. Loscalzo, J., Weinfeld, M., Fless, G.M., and Scanu, A.M. (1990) *Arteriosclerosis* 10:240-245.

8. Scanu, A.M., and Fless, G.M. (1990) *J. Clin. Invest.* 85:1709-1715.

9. Fless, G.M., ZumMallen, M.E., and Scanu, A.M. (1985) *J. Lipid Res.* 26:1224-1229.

10. Fless, G.M., ZumMallen, M.E., Scanu, A.M. (1986) *J. Biol. Chem.* 261:8712-8718.

11. Nielsen, L.B. (1999) *Atherosclerosis* 143:229-243.

12. Chen, S-H., Yang, C-Y., Chen, P-F., Setzer, D., Tanimura, M., Li, W-H., Gotto, A.M., and Chan, L. (1986) *J. Biol. Chem.* 261:12918-12921.

13. Chan, L. (1992) *J. Biol. Chem.* 267:25621-25624.

14. Walsh, M.T., and Atkinson, D. (1990) *J. Lipid Res.* 31:1051-1062.

15. Yang, C-Y., Kim, T.W., Weng, S-A., Lee, B., Yang, M., and Gotto Jr., A.M. (1990) *Proc. Natl. Acad. Sci. USA.* 87:5523-5527.

16. Coleman, R.D., Kim, T.W., Gotto Jr., A.M., and Yang, C-Y. (1990) *Biochim. Biophys. Acta.* 1037:129-132.

17. Sommer, A., Gorges, R., Kostner, G.M., Paltauf, F., and Hermetter, A. (1991) *Biochemistry* 30:11245-11249.

18. Albers, J.J., Kennedy, H., and Marcovina, S.M. (1996) *J. Lipid Res.* 37:192-196.

19. Rath, M., Niendorf, A., Reblin, T., Dietel, M., Krebber, H.J., and Beisiegel, U. (1989) *Arteriosclerosis* 9:579-592.

20. Niendorf, A., Rath, M., Wolf, K., Peters, S., Arps, H. Beisiegel, U., and Dietel, M. (1990) *Virchows Arch.* 417:105-111.

21. Reblin, T., Meyer, N., Labeur, C., Henne-Bruns, D., and Beisiegel, U. (1995) *Atherosclerosis* 113:179-188.

22. Utermann, G., Kraft, H.G., Menzel, H.J., Hopferwieser, T., and Seitz, C. (1988) *Hum. Genet.* 78:41-46.

23. Kark, J.D., Sandholzer, C., Friedlander, Y., and Utermann, G. (1993) *Atheriosclerosis* 98:139-151.

24. Seed, M., Hopplicher, F., Reaveley, D., McCarthy, S., and Thompson, G.R. (1990) *N. Engl. J. Med.* 322:1494-1499.

25. Guo, H.C., Chapman, M.J., Bruckert, E., Farriaux, J.P., and DeGennes, J.L. (1991) *Atherosclerosis* 86:69-83.

26. Goldstein, J.L., Ho, Y.K., Basu, S.K., and Brown, M.S. (1979) *Proc. Natl. Acad. Sci. USA.* 76:333-337.

27. Aqel, N.M., Ball, R.Y., Waldman, H., and Mitchinson, M.J. (1984) *Atherosclerosis* 53:265-271.

28. Steinberg, D., Parthasarathy, S., Carew, T.E., Khoo, J.C., and Witztum, J.L. (1989) *N. Engl. J. Med.* 320:915-924.

29. McLean, J.W., Tomlinson, J.E., Kuang, W-J., Eaton, D.L., Chen, E.Y., Fless, G.M., Scanu, A.M., and Lawn, R.M. (1987) *Nature* 330:132-137.

30. Hoover-Plow, J.L., Miles, L.A., Fless, G.M., Scanu, A.M., and Plow, E.F. (1993) *Biochemistry* 32:13681-13687.

31. Sangrar, W., Marcovina, S.M., and Koschinsky, M.L. (1994) *Prot. Eng.* 7:723-731.

32. Sangrar, W., Bajzar, L., Nesheim, M.E., and Koschinsky, M.L. (1995) *Biochemistry* 34:5151-5157.

33. Harpel, P.C., Gordon, B.R., and Parker, T.S. (1989) *Proc. Natl. Acad. Sci. USA.* 86:3847-3851.

34. Palabrica, T.M., Liu, A.C., Aronovitz M.J., Furie, B., Lawn, R.M., and Furie, B.C. (1995) *Nat. Med.* 1:256-259.

35. Kojima, S., Harpel, P.C., and Rifkin, D.B. (1991) *J. Cell Biol.* 113:1439-1445.

36. Grainger, D.J., Kirschenlohr, H.L., Metcalfe, J.C., Weissberg, P.L., Wade, D.P., and Lawn, R.M. (1993) *Science* 260:1655-1658.

37. Tomlinson, J.E., McLean, J.W., and Lawn, R.M. (1989) *J. Biol. Chem.* 264:5957-5965.

38. Koschinsky, M.L., Tomlinson, J.E., Zioncheck, T.F., Schwartz, K., Eaton, D.L., and Lawn, R.M. (1991) *Biochemistry* 30:5044-5051.

39. White, A.L., and Lanford, R.E. (1995) *Curr. Opin. Lipidol.* 6:75-80.

40. Gaws, A., and Hobbs, H.H. (1994) *Curr. Opin. Lipidol.* 5:149-155.

41. Gabel, B.R., and Koschinsky, M.L. (1995) *Biochemistry* 34:15777-15784.

42. Eaton, D.L., Fless, G.M., Kohr, W.J., McLean, J.W., Xu, Q-T., Miller, C.G., Lawn, R.M., and Scanu, A.M. (1987) *Proc. Natl. Acad. Sci. USA.* 84:3224-3228.

43. Haibach, C., Kraft, H.G., Köchl, S., Abe, A., and Utermann, G. (1998) *Gene* 208:253-258.

44. Scanu, A.M., and Edelstein, C. (1995) *Biochim. Biophys. Acta.* 1256:1-12.

45. Brunner, C., Kraft, H.G., Utermann, G., and Müller, H-J. (1993) *Proc. Natl. Acad. Sci. USA.* 90:11643-11647.

46. Koschinsky, M.L., Côté, G.P., and van der Hoek, Y.Y. (1993) *J. Biol. Chem.* 268:19819-19825.

47. Kratzin, H., Armstrong, V.W., Niehaus, M., Hilschmann, N., and Seidel, D. (1987) *Biol. Chem. Hoppe-Seyler* 368:1533-1544.

48. White, A.L., Rainwater, D.L., and Lanford, R.E. (1993) *J. Lipid Res.* 34:509-517.

49. Scanu, A.M., Miles, L.A., Fess, G.M., Pfaffinger, D., Eisenbart, J., Jackson, E., Hoover-Plow, J.L., Brunck, T., and Plow, E.F. (1993) *J. Clin. Invest.* 91:283-291.

50. Leerink, C.B., Duif, P.F.C.C.M., Gimpel, J.A., Kortlandt, W., Bouma, B.N., and van Rijn, H.J.M. (1992) *Thromb. Haemostasis* 68:185-188.

51. Chenivesse, X., Huby, T., Wickins, J., Chapman, J., and Thillet, J. (1998) *Biochemistry* 37:7213-7223.

52. Ernst, A., Helmhold, M., Brunner, C., Pethö-Schramm, A., Armstrong, V.W., and Müller, H-J. (1995) *J. Biol. Chem.* 270:6227-6234

53. Trieu, V.N., and McConathy, W.J. (1995) *J. Biol. Chem.* 270:15471-15474.

54. Gabel, B.R., May, L.F., Marcovina, S.M., and Koschinsky, M.L. (1996) *Arterioscler. Thromb. Vasc. Biol.* 16:1559-1567.

55. Boström, K., Borén, J., Wettesten, M., Sjöberg, A., Bondjers, G., Wiklund, O., Carlsson, P., and Olofsson, S-O. (1988) *J. Biol. Chem.* 263:4434-4442.

56. Borén, J., Graham, L., Wettesten, M., Scott, J., White, A., and Olofsson, S-O. (1992) *J. Biol. Chem.* 267:9858-9867.

57. Kraft, H.G., Menzel, H.J., Hoppichler, F., Vogel, W., and Utermann, G. (1989) *J. Clin. Invest.* 83:137-142.

58. Bonen, D.K., Hausman, A.M.L., Hadjiagapiou, C., Skarosi, S.F., and Davidson, N.O. (1997) *J. Biol. Chem.* 272:5659-5667.

59. Wilkinson, J., Munro, L.H., and Higgins, J.A. (1994) *J. Lipid Res.* 35:1896-1901.

60. White, A.L., and Lanford, R.E. (1994) *J. Biol. Chem.* 269:28716-28723.

61. Wang, L., Fast, D.G., and Attie, A.D. (1997) *J. Biol. Chem.* 272:27644-27651.

62. Terada, K., Manchinkalapudi, P., Noiva, R., Jauregui, H.O., Stockert, R.J., and Schilsky, M.L. (1995) *J. Biol. Chem.* 270:20410-20416.

63. Rudel, L.L., Newton, R., Hamilton Jr, R., Deckelbaum, R.J., and Hobbs, H.H. (1994) *J. Lipid Res.* 35:1122-1128.

64. Frank, S., Durovic, S., Kostner, F., and Kostner, G.M. (1995) *Arterioscler. Thromb. Vasc. Biol.* 15:1774-1780.

65. Phillips, M.L., Lembertas, A.V., Schumaker, V.N., Lawn, R.M., Shire, S.J., and Zioncheck, T.F. (1994) *Chem. Phys. Lipids* 68:91-97.

66. Koschinsky, M.L., Marcovina, S.M., May, L.F., and Gabel, B.R. (1997) *Clin. Genet.* 52:338-346.

67. Guevara Jr, J., Spurlino, J., Jan, A.Y., Yang, C-Y., Tulinsky, A., Prasad, B.V.V., Gaubatz, J.W., and Morrisett, J.D. (1993) *Biophys. J.* 64:686-700.

68. McCormick, S.P., Ng, J.K., Taylor, S., Flynn, L.M., Hammer, R.E., and Young, S.G. (1995) *Proc. Natl. Acad. Sci. USA.* 92:10147-10151.

69. Callow, M.J., and Rubin, E.M. (1995) *J. Biol. Chem.* 270:23914-23917.

70. Gabel, B.R., Yao, Z., McLeod, R.S., Young, S.G., and Koschinsky, M.L. (1994) *FEBS Letters* 350:77-81.

71. Chiesa, G., Hobbs, H.H., Koschinsky, M.L., Lawn, R.M., Maika, S.D., and Hammer, R.E. (1992) *J. Biol. Chem.* 267:24369-24374.

72. Callow, M.J., Stoltzfus, L.J., Lawn, R.M., Maika, S.D., and Rubin, E.M. (1994) *Proc. Natl. Sci. USA* 91:2130-2134.

73. Gabel, B.R., McLeod, R.S., Yao, Z., and Koschinsky, M.L. (1998) *Arterioscler. Thromb. Vasc. Biol.* 18:1738-1744.

74. Rahman, M., Jia, Z., Gabel, B.R., Marcovina, S.M., and Koschinsky, M.L. (1998) *Prot. Eng.* 11:1249-1256.

75. Frank, S., Durovic, S., and Kostner, G.M. (1994) *Biochem. J.* 304:27-30.

76. Gabel, B.R., and Koschinsky, M.L. (1998) *Biochemistry* 37:7892-7898.

77. Kostner, G.M., Wo, X., Frank, S., Kostner, K., Zimmermann, R., and Steyrer, E. (1997) *Clin. Genet.* 52:347-354.

78. Suva, L.J., Winslow, R.E.H., Wettenhall, R.G., Hammonds, G.M., Moseley, H., Diefenbach-Jagger, H., Rodda, C.P., Kemp, B.E., Rodriguez, H., Chen, E.Y., Hudson, P.J., Martin, T.J., and Wood, W.I. (1987) *Science* 237:893-896.

79. Keesler, G.A., Gabel, B.R., Devlin, C.M., Koschinsky, M.L., and Tabas, I. (1996) *J. Biol. Chem.* 271:32096-32104.

80. Graham, F.L., and van det Eb, A.J. (1973) *Virology* 52:456-467.

81. Gorman, C., Padmanahban, R., and Howard B. (1983) *Science* 221:551-553.

82. Laemmli, U.K. (1970) *Nature* 227:680-685.

83. Havel, R.J., Eder, H.A., and Bragdon, J.D. (1955) *J. Clin. Invest.* 34:1345-1353.

84. Frank, S., and Kostner, G.M. (1997) *Prot. Eng.* 10:291-298.